TLR4 regulation in human fetal membranes as an explicative mechanism of a pathological preterm case.

Corinne Belville[1], Flora Ponelle-Chachuat[1], Marion Rouzaire[1], Christelle Gross[1], Bruno Pereira[2], Denis Gallot[1, 3], Vincent Sapin[1, 4], Loïc Blanchon[1].

Author affiliation:

1. Team "Translational approach to epithelial injury and repair," GReD, Université Clermont Auvergne, UMR6293 CNRS-U1103 INSERM, F-63000 Clermont-Ferrand, France.
2. CHU Clermont-Ferrand, Biostatistics unit (DRCI) Department, F-63000 Clermont-Ferrand, France.
3. CHU Clermont-Ferrand, Obstetrics and Gynecology Department, F-63000 Clermont-Ferrand, France.
4. CHU Clermont-Ferrand, Biochemistry and Molecular Genetic Department, F-63000 Clermont-Ferrand, France.

Corresponding author: Dr Loic Blanchon, UFR de Médecine et des Professions Paramédicales, Bâtiment CRBC, GReD, TSA 50400, 28 place Henri-Dunant, F63001 Clermont-Ferrand Cedex 1, France, Tel: +33 4 73 17 81 74, e-mail: loic.blanchon@uca.fr

Short Title: TLR4 control upon fetal membrane rupture

Keywords: fetal membranes rupture / methylome / miRNA / transcriptome / TLR4

Word count: Abstract: 179

ABSTRACT

The integrity of human fetal membranes is crucial for harmonious fetal development throughout pregnancy. Their premature rupture is often the consequence of a physiological phenomenon previously exacerbated. Beyond all biological processes implied, inflammation is of primary importance and is qualified as "sterile" at the end of pregnancy. Complementary methylomic and transcriptomic strategies on amnion and choriodecidua explants taken from the altered (cervix zone) and intact fetal membranes at term and before labor were used in this study. By cross-analyzing genome-wide studies strengthened by *in vitro* experiments, we deciphered how the expression of Toll-like receptor 4 (TLR4), a well-known actor of pathological fetal membrane rupture, is controlled. Indeed, it is differentially regulated in the altered zone and between both layers by a dual mechanism: 1) the methylation of TLR4 and miRNA promoters and 2) targeting by miRNA (let-7a-2 and miR-125b-1) acting on the 3'-UTR of TLR4. Consequently, this study demonstrates that a fine regulation of TLR4 is required for sterile inflammation establishment at the end of pregnancy and that it may be dysregulated in the pathological premature rupture of membranes.

48 **INTRODUCTION**

49 Placenta and fetal membranes are extra-embryonic tissues originally formed by
50 trophoblastic cell differentiation. Although these organs are transitory, their integrities
51 throughout pregnancy are essential for harmonious *in-utero* fetal development. Protecting the
52 fetus (considered a semi-allogeneic graft), fetal membranes are composed of amnion and
53 chorion, creating a 0.5 mm-thick layer surrounding the amniotic cavity. They are important for
54 the protection of the fetus against infections ascending the genital tract and for the initiation of
55 programmed term rupture (Joyce *et al*, 2009; Kendal-Wright, 2007). The site of rupture is a
56 particular and unique zone of altered morphology (ZAM) situated around the cervix (McLaren
57 *et al*, 1999; McParland *et al*, 2003), which along with a zone of intact morphology (ZIM)
58 presents specific histological characteristics involving a substantial reduction of both layer
59 thickness and cellular apoptosis (El Khwad *et al,* 2006) decreased the adherence of the amnion
60 and the choriodecidua; the appearance of a swollen, spongy layer between them (Mauri *et al*,
61 2013) and epithelial to mesenchymal transition (EMT) (Silva *et al*, 2020). The evident global
62 regional disorganization is principally a consequence of neutrophil and macrophage migrations
63 (Osman *et al*, 2006) and collagen remodeling, which are essentially linked to an increased
64 activity of matrix metalloproteinases (MMP) (McLaren *et al*, 2000). Furthermore, the release
65 of pro-inflammatory cytokines due to innate immunity activates global inflammatory pathways,
66 usually referred to as "sterile inflammation" (Gomez-Lopez *et al*, 2014). A sequential scenario
67 occurs with the first chorion's breaking, amnion invagination, and rupture (Gillaux *et al*, 2011).

68 Dysregulation of fetal membrane's integrity or a premature activation of inflammatory
69 pathways could lead to preterm premature rupture of membranes (PPROM). This is associated
70 with a high mortality rate and significant morbidity in newborn survivors due to fetal
71 prematurity and maternal complications (Goldenberg *et al*, 2008). Such pathology, affecting
72 the amnion and chorion before 37 weeks of gestation, accounts for approximatively 30% of

73 premature deliveries and 1–3 % of all births (Waters & Mercer, 2011). Deregulated genes (e.g.,
74 MMP1, ITGA11, and THBS2; (Wang *et al*, 2008; Yoo *et al*, 2018) miRNA, (Enquobahrie *et*
75 *al*, 2016), and long chain non-coding RNA (lncRNA) (Luo *et al*, 2013)) expressions were
76 demonstrated to correlate with PPROM appearance by affecting different biological pathways.
77 Several causes have been found to increase the incidence of this pathology, where
78 microorganisms ascending and invading the intra-amniotic cavity appear to be one of the most
79 important explanations (Konwar *et al*, 2018; Musilova *et al*, 2015; Romero *et al*, 2006a). This
80 leads to chorioamnionitis, triggering an early and acute inflammatory response and implying
81 the involvement of intracellular or surface-expressed pattern recognition receptors (PRRs) as
82 innate components of the immune system, including the most frequently described toll-like
83 receptor (TLR) family (Kawai & Akira, 2010; Newton & Dixit, 2012).

84 To better understand the physiological and pathological rupture of membranes, the
85 molecular study of global changes in gene expression can be accomplished using high-scale
86 technics analyses. Only 12 % of the studies concerning gestational tissues have used fetal
87 membranes. Furthermore, only 5 % investigated healthy pregnancies, whereas a physiological
88 case could undoubtedly serve as an image of a premature exacerbated phenomenon in a
89 pathological case. Ninety percent were conducted on pathological pregnancies, with 31 %
90 specifically involving PPROM (Eidem *et al*, 2015). In term delivery, several researchers have
91 observed an acute inflammatory signature in fetal membranes under different conditions: labor
92 versus no labor (Haddad *et al*, 2006) in the placental amnion versus the reflected amnion with
93 labor (Han *et al*, 2008) and in the choriodecidua (Stephen *et al*, 2015). Using human primary
94 amnion mesenchymal cells treated with IL-1β, an elegant model of sterile inflammation
95 (rapidly-activated by NF-κB responsive genes) was found to be associated with an
96 inflammatory cascade (Li *et al*, 2011; Lim *et al*, 2012). Thus, in the ZAM, the sterile
97 inflammation and/or extracellular matrix (ECM) remodeling and disorganization absolutely

98 depends on global gene expression profiles in the amnion and the chorion. Surprisingly, only
99 one unique transcriptome study focused on the ZIM or ZAM regions and amnion and chorion
100 tissues, characterizing a specific differential expression in a spontaneous rupture at term with
101 labor. Differences were observed in the chorion, though not in the amnion, specifically
102 involving biological processes, such as extracellular matrix-receptor interaction and
103 inflammation (Nhan-Chang *et al*, 2010). In addition to classical direct gene regulation by
104 transcription factors, DNA methylation is another well-known epigenetic mechanism that can
105 interfere with the transcriptional regulation of all RNA types (Kim *et al*, 2009). Concerning a
106 physiological rupture, the differential methylation study regarding fetal membranes only
107 focused on the amnion. Genome-wide methylation differed between the labor and non-labor
108 groups at different pregnancy terms, particularly affecting the genes involved in cytokine
109 production and gated channel activity, among others (Kim *et al*, 2013).

110 Because little is known about biochemical changes at term without labor (not influenced
111 by mechanical stress) with regard to physiological conditions at the site of rupture (ZAM) and
112 away from the site (ZIM), the purpose of our study was to exhaustively combine and correlate
113 methylomic and transcriptomic analyses. We hypothesized that by cross-analyzing our genome-
114 wide studies, we could explain the different levels of gene expression by comparing the
115 amnion/choriodecidua and the ZIM/ZAM. After classifying genes into specific biological
116 processes, we focused our study on inflammation. Under conditions at term without labor, we
117 demonstrated that toll-like receptor 4 (TLR4), classically involved in the recognition of *E.coli*
118 and triggering an inflammatory response in chorioamnionitis leading to PPROM (Medzhitov *et*
119 *al*, 1997; Poltorak *et al*, 1998), was overexpressed in the ZAM choriodecidua compared to the
120 ZAM amnion. Furthermore, we discovered that TLR4 regulation leads to layer and zone
121 specificity. The latter occurred due to the hypomethylation of the TLR4 gene body in the ZAM
122 choriodecidua, whereas its weak expression in the ZAM amnion layer was a direct consequence

of the action of two hypomethylated miRNAs targeting the 3-UTR of TLR4: let-7a-2 and miR-125b-1. Therefore, the physiological choriodecidual over-expression of TLR4 could be exacerbated in PPROM, leading to the enhancement of the first step of an early scenario of a fetal membrane rupture.

128 **RESULTS**

129 **The methylomic analysis of fetal membranes allows for defining the gene ontology**
130 **classification for the ZAM zone**

131 After identifying the differentially hypermethylated genes between the amnion and the
132 choriodecidua on the whole genome between the ZIM and ZAM (Figure 1A), a biological
133 process analysis was performed and represented by a four-way Venn diagram (Figure 1B). If
134 the hypermethylated genes were clearly lower in the ZIM (1,746 genes) than the ZAM (9,830
135 genes), the specific genes only found in the ZIM (hyper- or hypomethylated; total number 98
136 [i.e., 10 + 88, illustrated by black circles]) did not exhibit any statistically significant result (p-
137 value < 0.01 with a Bonferroni correction). In contrast, the specific genes modified in terms of
138 methylation for the ZAM (total number 5,750 [i.e., 3,379 + 2,371, illustrated by white circles])
139 led to the discovery of the numerous biological processes detailed in Figure 1C. Precisely, the
140 number of characterizations of an enrichment in GO term IDs were clearly more concentrated
141 and were thus more biologically significant in the case where a definite gene was more
142 methylated in the amnion than in the choriodecidua (mA > mC). The biological process term
143 IDs containing the most important gene number were the G-protein coupled receptor signaling
144 pathways (such as for defense response, detection of stimulus, or inflammatory response),
145 which could be linked to sterile inflammation and to the onset of parturition related to fetal
146 membrane ruptures.

147

148 **The transcriptomic analysis of fetal membranes in the ZAM zone is more relevant for**
149 **downregulated genes in the amnion compared to the choriodecidua**

150 To supplement the results obtained from the methylome analysis, a transcriptomic study
151 using the same samples was performed for the ZAM to compare the difference in gene

152 expression between the amnion and the choridecidua. We observed that 501 and 145 genes
153 specific to the ZAM were respectively down- and upregulated when the expression levels were
154 compared between the amnion and the choriodecidua (a log2 fold change [FC] cut-off lower or
155 higher than 2.8 [Figure 2, middle panel, supplementary Table S3]).

156 The processes seemed to be more relevant and specific when the genes less expressed
157 in the amnion than in the choriodecidua (i.e., log2 FC < 2.8) were considered. Indeed, genes
158 could be grouped into two relevant GO terms: *response to external stimulus* and *female*
159 *pregnancy* (Figure 2, top panel). In the case where genes were more expressed in the amnion
160 than in the choriodecidua (i.e., log2 FC > 2.8), the biological processes exhibited no statistically
161 significant result (p-value < 0.01 with a Bonferroni correction). The analyses undertaken with
162 uncorrected p-values did not provide relevant information because conventional tissue
163 development or ossification were observed (Figure 2, bottom panel).

164

165 **Combination of transcriptomic and methylomic results in the ZAM zone demonstrate that**
166 **genes more expressed in the choriodecidua are linked to pregnancy pathologies**

167 By cross-analyzing the results obtained from the two preceding analyses (methylome
168 and transcriptome), a total of 26 genes were hypermethylated in the choriodecidua, and more
169 were expressed in the amnion (supplementary Table S4). The biological process (GO term)
170 analysis was not significant, which is likely due to the small number of studied genes and the
171 fact that the underlying generic processes were linked only to urogenital abnormalities and not
172 to pathological pregnancy, as confirmed by the MeSH disease terms (supplementary Table S5).

173 Conversely, 105 genes were hypermethylated in the amnion and were more expressed
174 in the choriodecidua (Figure 3A and supplementary Table S6). They could be classified in
175 MeSH disease terms linked directly to pregnancy pathologies, such as placenta diseases

176 (trophoblastic neoplasms, pre-eclampsia, fetal growth retardation, or placenta accreta), female
177 urogenital diseases, and pregnancy complications (supplementary Table S7). The GO term
178 analysis clearly identified three complementary pathways: response to external stimulus,
179 detection of LPSs, and inflammatory response. Interestingly, fetal membranes were sensitive to
180 an external stimulus, such as Gram-negative bacterial molecules and LPSs, in relation to the
181 inflammatory response. Of all the genes classified in these processes, TLR4 was the only one
182 represented in all these biological processes and therefore seems to play a central role in
183 parturition at term. To validate our *in-silico* observations and to pave the way for describing
184 TLR4's importance, immunofluorescence experiments were first conducted to confirm such a
185 protein's presence in the amnion and the choriodecidua of the ZAM (Figure 3B). Moreover, we
186 established the ability of the choriodecidua and the amnion to respond to TLR4 activation after
187 the binding of its natural ligand (LPS) by secreting IL-6 and TNF-α proteins in the culture
188 medium (Figure 3C). Considering the important role of TLR4 in sterile or pathological
189 inflammation (chorioamnionitis), the remainder of the study focused on the characterization
190 and regulation of TLR4 expression in fetal membranes, as ascertained by the cross-analysis of
191 the methylomic and transcriptomic results.

192

193 **The tissue specificity of TLR4 regulation at the end of pregnancy in the weak ZAM is due**
194 **to hypermethylation in the amnion**

195 Focusing on the TLR4 genomic zone, five cytosines distributed on the promoter, body,
196 and UTR were studied using a methylomic array. The statistical study of the cytosine
197 methylation β-values of the nine genomic DNA samples demonstrated that the five were
198 hypermethylated in the amnion compared to the choriodecidua (Figure 4A). These results were
199 confirmed by the bisulphite treatment and enzymatic digestion (taking advantage of the Taq I

200 restriction site present only in this CpG zone) of the amnion and choriodecidua samples with a
201 focus on only one cytosine: cg 05429895 (Figure 4B). Furthermore, of the nine RNA samples,
202 the link between methylation and expression revealed by the methylomic and trancriptomic
203 arrays was confirmed by qRT-PCR (Figure 4C) and Western blot (Figure 4D) analyses,
204 showing a higher expression of TLR4 in the choriodecidua than in the amnion.

205

206 **The tissue specificity of TLR4 regulation could be due to miRNA action**

207 Because gene expression can be also regulated post-transcriptionally by the action of
208 mi-RNA, it would be interesting to perform an *in-silico* analysis of differentially methylated
209 miRNA (linked to TLR4) between the amnion and the choriodecidua. The results showed that
210 two of them (let-7a-2 and miR-125b-1) could target the 3'UTR region of TLR4 mRNA (Figure
211 5A). Focusing on these two, all the cytosines studied on the methylomic chip were situated in
212 the 5' upstream sequence of miRNA. Five of six were statistically significant for over-
213 methylation in the choriodecidua compared to the amnion for miR-125b-1 and for the unique
214 one in, let-7a-2 (Figure 5B up and bottom panel). Using the same samples that were previously
215 used for the quantification of mRNA TLR4, the expression of each pri-miRNA by the qRT-
216 PCR was checked. As expected, an overexpression of pri-miR-125b-1 was observed in the
217 amnion compared to the choriodecidua. A weak basal expression level below the detection limit
218 of the qPCR assay for pri-let-7a-2 did not allow for obtaining results that could reasonably be
219 analyzed (Figure 5C).

220

221 **let-7a-2 and miR-125b-1 target the 3'-UTR-TLR4**

222 We first established that in the human cell line HEK293 (classically used in a gene
223 reporter assay for testing miRNA targets), both miRNAs could decrease the amount of

224 luciferase by targeting the 3'-UTR region of TLR4 mRNA (Figure 6A). To choose a better
225 cellular model to test this miRNA action linked with the fetal membrane environment, the
226 relative amount of TLR4 mRNA was determined in various human amniotic cells. Figure 6B
227 demonstrates that AV3 (one of the three tested amniocyte cell lines, compared to FL and WISH)
228 was the most efficient, and it was therefore used for the following experiments. For *in vitro* or
229 physiological models, AV3 and primary amniotic epithelial cells were respectively used to
230 confirm that both miRNAs clearly targeted TLR4 mRNA or protein accumulation (Figure 6C
231 and 6D). For the AV3 cell line, a significant decrease of the mRNA amount was observed from
232 12 h after the transfection of let-7a-2 and miR-125b-1 or the co-transfection of let-7a-2+ miR-
233 125b-1. This effect persisted only for let-7a-2 at 24 h, confirming the quick action of this
234 cellular system. Furthermore, after 24 h of transfection, a decrease in the TLR4 protein amount
235 was significantly demonstrated for let-7a-2 and after 48 h for miR-125b-1 or both transfections
236 of let-7a-2 + miR-125b-1. The use of primary cells confirmed this physiological action with a
237 decrease in the TLR4 mRNA amount at 48 h after the transfection of miR-125b-1 and co-
238 transfection of let-7a-2 + miR-125b-1 and after 72 h for the TLR4 protein for the three
239 conditions.

240

241 **DISCUSSION**

242 Worldwide, preterm birth is a serious medical problem, particularly regarding the long-
243 term consequences throughout the entire life of premature infants. PPROM represents one-third
244 of pregnancies that end prematurely and is found to be principally dependent on an early scale
245 and the kinetic activation of inflammation, signaling a cascade in gestational tissues.

246 Because the inflammatory mechanisms of preterm and term birth are broadly similar,
247 understanding how human fetal membranes are prepared for their physiological rupture is
248 essential. Studies have been partially documented and establish that a weak zone (ZAM)
249 situated in the cervix zone emerged at the end of the nine month of the gestation period
250 (McLaren *et al*, 1999) as a direct consequence of global layer disorganization and weakening.
251 All these phenomena are key determinants of a rupture and could be directly linked to a
252 common denominator: the regulation and modification of gene expression levels (Romero *et*
253 *al*, 2006b). For the first time, a complementary high-throughput approach was applied by
254 performing both transcriptomic and methylomic analyses on the same samples. Moreover, the
255 strength of this work is to highlight both the global geographical (ZIM/ZAM) and tissue layer
256 (amnion vs. choriodecidua) differences in terms of DNA methylation and gene expression.
257 Indeed, our methylomic study established a global profile of fetal membranes on the ZIM and
258 ZAM samples. The number of hypermethylated genes in the amnion or the choriodecidua were
259 more important in the ZAM than in the ZIM and allowed us to perform a GO-term classification
260 focused on the ZAM, where cell adhesion, response to a stimulus, tissue development, and
261 reproductive processes are significantly represented. We found some similarities with the
262 transcriptomic analysis, where overexpressed genes in the choriodecidua ZAM were linked to
263 biological adhesion (important in tissue integrity), regulation of cell proliferation, extracellular
264 matrix organization, and responses to internal and external stimuli.

265 By cross-analyzing both methods for the ZAM, the link of 105 genes overexpressed in
266 the choriodecidua and hypomethylated in the amnion with a MeSH disease terms (e.g.,
267 pregnancy complication) was revealed. Especially for GO terms, these highlighted processes
268 could be directly linked to preparation for parturition through a sterile inflammation cascade.
269 We then turned our attention to TLR4, a major mediator of inflammation, for the following
270 reasons. First, this upstream gatekeeper of innate immune activation was the only gene that
271 appeared in each of the considered GO terms, as illustrated in Figure 3A. Second, it is an
272 important partner of many other genes included in our 105 genes list (see Figure 3B). Third,
273 TLR4 was already known to be expressed in the fetal membranes and cervices of animals
274 (Gonzalez *et al*, 2007; Harju *et al*, 2005; Moço *et al*, 2013) and to play a role as a key regulator
275 in a sterile or septic inflammatory reaction in response to aggression by a pathogen-associated
276 molecular pattern (PAMP)/damage-associated molecular pattern (DAMP), leading to PPROM
277 (Chin *et al*, 2016; Li *et al*, 2010; Patni *et al*, 2007; Wang & Hirsch, 2003). Fourth, TLR4 is also
278 known to be involved in parturition at the classical term of pregnancy, activating a sterile
279 inflammation cascade (Choi *et al*, 2012; Wahid *et al*, 2015). Fifth, it could be considered a
280 promising therapeutical target to prevent preterm birth through a better control of its pro-
281 inflammatory signaling.

282 According to a previous study (Krol *et al*, 2010), and as confirmed by our qPCR and
283 Western blot quantification, TLR4 was more expressed in the choriodecidua than in the amnion
284 (Figure 4B and 4C). This overexpression could be due to a differential methylation and/or
285 transcription factor fixations or could be a consequence of post-transcriptional regulation by
286 miRNAs. miRNAs play crucial regulatory roles in biological and pathological processes. They
287 are well-documented in gestational tissues, such as the placenta, endometrium, and fetal
288 membranes (Doridot *et al*, 2014; Gu *et al*, 2013; Kamity *et al*, 2019; Montenegro *et al*, 2007;
289 Wang *et al*, 2016). They have actually begun to be considered potential biomarkers for

290 pregnancy pathologies (Cretoiu *et al*, 2016), and studies have already shown that some miRNA
291 expressions decrease in chorioamniotic membranes with gestational age uninfluenced by labor
292 (Montenegro *et al*, 2007, 2009). We found two miRNAs (mir-125b-1 and let-7a-2) that were
293 hypermethylated in the choriodecidua compared to the amnion that could potentially target
294 TLR4 mRNA in the amnion to decrease its expression level. They were never known to be able
295 to specifically target TLR4, leading us to demonstrate the consequences of their transfection on
296 the quantification of the TLR4 mRNA and protein on the cell line AV3 or primary amniotic
297 epithelial cells using the luciferase 3'UTR of the TLR4 reporter gene.

298 Surprisingly, these two miRNAs are part of a miR-100-let-7a-2 cluster host gene, also
299 known as MIR100HG. This cluster has never been studied in relation to the placenta or fetal
300 membrane environment, unlike others, such as C14MC, C19MC, and miR-371-3, whose
301 expressions change during pregnancy between the whole and terminal villi (Gu *et al*, 2013;
302 Morales-Prieto *et al*, 2013). In humans, 10 mature let-7s are synthetized and are implicated in
303 different physiological and pathological events from embryogenesis to adult development, such
304 as inflammatory responses and innate immunity (Roush & Slack, 2008); however, the latter
305 finding could not be linked only to simple TLR4 targeting because both miRNAs were also
306 already known to have implications for innate immunity by influencing not only the expression
307 of interleukins and TNFα but also cell senescence—another well-known phenomenon
308 occurring at the end of fetal membrane life (Iliopoulos *et al*, 2009; Nyholm *et al*, 2014; Schulte
309 *et al*, 2011; Tili *et al*, 2007).

310 On a global scale, the exhaustive results obtained here provide causal information
311 regarding the implication of inflammation in the physiological rupture of fetal membranes,
312 whereas future studies are needed to exploit all the data accumulated during this work.
313 Nevertheless, by focusing on a unique candidate, TLR4, a well-known actor in the physiological
314 and pathological rupture of membranes, we have outlined the complex molecular process of

315 gene regulation and have proposed a fetal membrane layer-specific model to better understand
316 fetal membrane ruptures (Figure 7). The latter could doubtlessly be extrapolated to other
317 gestational tissues or resident immune cells, such as neutrophils, which are implicated in the
318 amplification of the inflammatory response in late gestation. Moreover, this scheme shows that
319 TLR4 could be an attractive drug target for prolonged gestation and could protect the fetus
320 against inflammatory stress (Robertson *et al*, 2020).

321 All together, these data allow for the expectation of the emergence and promising
322 clinical strategies for pregnant women to prevent PPROM, which will undoubtedly come from
323 results such as ours regarding the physiological preparation of fetal membrane ruptures at term.
324
325

326 **MATERIALS AND METHODS**

327 **Ethics statements**

328 This study was approved by the regional institutional ethics committee, and informed
329 consent was obtained from the participants. The experiments conformed to the principles set
330 out in the World Medical Association Declaration of Helsinki.

331

332 **Human fetal membrane collection**

333 Nine fetal membranes were collected at full term before labor and birth by cesarean
334 section (Obstetrics Department, Estaing University Hospital, Clermont-Ferrand, France). All
335 patients were Caucasian and presented no pregnancy pathology (confirmed by macroscopic and
336 microscopic placenta analyses and histological examinations that excluded chorioamnionitis).
337 Supplementary Table S1 describes the patients' characteristics.
338 Four samples were collected from each patient (ZAM amnion, ZAM choriodecidua,
339 ZIM amnion, and ZIM choriodecidua) as already described by Choltus *et al* (2020).

340 **Genome-wide DNA methylation**

341 Total genomic DNA from the amnion and choriodecidua was extracted using the
342 QIAamp® DNA Mini Kit (Qiagen, Courtaboeuf, France) following the manufacturer's
343 instructions. DNA concentration was determined by Qubit™ quantitation (Invitrogen, Thermo
344 Fisher Scientific, Illkirch, France). Five hundred ng of extracted DNA was bisulfite-treated
345 using the EZ DNA Methylation™ Kit (Proteigene, Saint-Marcel, France), following the
346 manufacturer's standard protocol, and individually hybridized using HumanMethylation450
347 Analysis BeadChip (Illumina, San Diego, California, USA), which allowed for studying the
348 482,421 cytosines on the human genome. This array was conducted using Helixio (Saint-

349 Beauzire, France). Specific CpG probe methylation differences between the tissues taken from
350 the ZIM and ZAM regions or between the amnion and choriodecidua were analyzed. To study
351 each cytosine, methylation differences were defined as a change in β values (Δβ) between two
352 conditions with p-values less than 0.05 (after applying a Student's paired t-test), and the Monte
353 Carlo method (Metropolis and Ulam, 1949) was then used to randomly stimulate the minimal
354 (m) and maximal (M) Δβ-value for each chromosome. Such limits permitted us to keep only
355 the cytosine in which Δβ was inferior to M or superior to M. Gene probes meeting the cut-off
356 criteria for each comparison were submitted for Database for Gene Ontology (GO) enrichment
357 (http://go.princeton.edu) in association with the REVIGO web server (http://revigo.irb.hr; as
358 previously described (Supek *et al*, 2011) to identify the biological processes associated with the
359 genes that showed changes in methylation status.

360

361 **Human 8x60K expression arrays**

362 Total RNA was extracted using an RNeasy® Mini Kit (Qiagen) following the
363 manufacturer's instructions. RNA samples were quantified with a NanoDrop™
364 spectrophotometer (ThermoScientific, Thermo Fisher Scientific, Illkirch, France). The RNA
365 integrity was evaluated using a 2100 Bioanalyzer (Agilent Technologies, Les Ullis, France) and
366 an RNA 6000 Nano Assay Kit. The mean of the RNA integrity number (RIN) for all samples
367 was 8.41.

368 A microarray (Sure Print G3 Human GE 8x60K) was performed by Helixio (Saint-
369 Beauzire, France) in accordance with Agilent Technologies. The data were analyzed with
370 Genespring GX 12.0 (Agilent Technologies).

371 The resulting gene lists from each pair-wise comparison (ZIM vs. ZAM and amnion vs.
372 choriodecidua) were respectively filtered for the genes that showed 2.8-fold changes at $p < 0.01$

373 using the Student–Newman–Keuls test with Benjamini–Hochberg corrections for false
374 discovery rates. Raw data were analyzed with the R (http://R-project.org) and Bioconductor
375 (http://www.bioconductor.org) software. A generic GO term finder (http://go.princeton.edu)
376 and REVIGO (http://revigo.irb.hr/) with up- and downregulated probes were used to analyze
377 the biological process of gene ontology (GO) enrichment, and GePS Genomatix software
378 (Release 2.4.0 Genomatix® Software GmbH, Munich, Germany) was used for the analysis of
379 MeSH diseases ($p < 0.01$).

380

381 **TLR4 immunofluorescent staining**

382 Immunohistochemistry experiments performed on ZAM cryosections taken from the
383 same samples (8 µm) were fixed in paraformaldehyde (4 % in PBS); blocked with PBS-1X,
384 Triton 0.1 %, and SVF 10%; and incubated overnight with a monoclonal mouse anti-TLR4
385 antibody diluted 1:400 in PBS (Sc-293072, Santa-Cruz Biotechnology, Dallas, Texas, USA).
386 A secondary antibody (donkey anti-mouse coupled with Alexia 488 Ig G [H+L]; Life
387 Technologies, Thermo Fisher Scientific) diluted at 1:300 was incubated for 2 h on slides.
388 Following Hoechst nuclear staining, the samples were examined under a LSM510 Zeiss
389 confocal microscope (Zeiss, Oberkochen, Germany). For negative controls, sections were
390 incubated without a primary antibody.

391

392 **Stimulation of fetal membrane explants by Lipopolysaccharide (LPS)**

393 Amnion and choriodecidua explants (2 cm^2) were placed in six-well plates with 2 ml of
394 DMEM/F12 (Gibco, Thermo Fisher Scientific) supplemented with 10 % fetal bovine serum
395 (FBS, GE Healthcare, Vélizy-Villacoublay, France), 100 units/ml of penicillin, 100 µg/ml of

396 Streptomycin, and 0.25 µg/ml of Amphotericin B (Hyclone, Thermo Fisher scientific) for 24 h.
397 The medium was then removed and replaced with serum-free DMEM/F12. The explants were
398 treated (or left untreated) with LPS from E.coli (O55:B5) at 0.5 µg/ml (Sigma-Aldrich Chimie,
399 St. Quentin Fallavier, France) for 24 h. The treated explants and cell-free culture medium were
400 collected and stored at -80 °C.

401

402 **Cytokine analysis**

403 Secreted IL-6 and TNFα cytokines were measured in an amnion and choriodecidua-
404 conditioned medium using a Bio-Plex Pro™ Human Cytokine 27-plex Assay (Bio-Rad, Marnes-
405 la-Coquette, France) as recommended by the manufacturer along with Luminex technology.
406 The results were standardized with the total protein concentration using a Pierce™ BCA Assay
407 (Thermo Fisher Scientific).

408

409 **Bisulfite conversion and combined restriction analysis**

410 Total DNA from the amnion and choriodecidua explants was bisulfite-treated using an
411 EZ DNA methylation kit (Zymo Research, Proteigene). The converted DNAs were used as
412 templates for the PCR reaction using specific primers of promoter TLR4 (containing the
413 cytosine cg 05429895; promot-F: 5' TTTAGAGAGTTATAAGGGTTATTT 3', and promot-
414 R: 5' CTAACA TCATCCT CACTACTTC 3'). The PCR was performed using HotStart DNA
415 Polymerase (Qiagen), and the products were digested with Taq I (New England Biolabs, Evry,
416 France) that could recognize CpGs. Digested products were analyzed on polyacrylamide gel.

417

418 **Cell cultures**

419 Primary amniocyte cells were collected from the amnion after trypsination and were
420 cultured on six-well plates coated with bovine collagen type I/III (StemCell Technologies,
421 Saint-Egrève, France) as described previously (Marceau *et al*, 2006; Prat *et al*, 2015). Human
422 embryonic kidney (HEK) 293 cells were grown in Dulbecco's Modified Eagle Medium
423 (DMEM; Gibco) supplemented with 10 % fetal bovine serum (FBS, GE healthcare), 4mM
424 glutamine (Gibco), 1mM sodium pyruvate (Hyclone), 1x non-essential amino acids (Gibco),
425 100 units/ml of penicillin, 100 µg/ml of Streptomycin, and 0.25 µg/ml of Amphotericin B
426 (Hyclone).

427 Human epithelial amnion cells (AV3 cells, ATCC-CCL21; FL, ATCC-CCL62; WISH,
428 ATCC-CCL25) were cultured in DMEM/F12 (Gibco) supplemented with 10 % fetal bovine
429 serum (FBS, GE healthcare), 4 mM glutamine (Gibco), 100 units/ml of penicillin, 100 µg/ml
430 of Streptomycin, and 0.25 µg/ml of Amphotericin B (Hyclone).

431

432 **Quantitative RT-PCR**

433 Total RNA was isolated from the amnion, choriodecidua, human epithelial amnion cells
434 (AV3, FL, and WISH), and primary amniocyte cells using an RNeasy® Mini Kit (Qiagen) with
435 DNAse I digestion as described in the manufacturer's protocol. After quantification with a
436 NanoDrop™ spectrophotometer (Thermo Fisher Scientific), cDNA was synthesized from 1µg
437 of RNA using a SuperScript™ III First-Strand Synthesis System for RT-PCR (Invitrogen,
438 Thermo Fisher Scientific). Quantitative RT-PCR reactions were performed with a LightCycler®
439 480 (Roche Diagnostics, Meylan, France) using Power SYBR® Green Master Mix (Roche) and
440 specific primers (described in supplementary Table S2). Transcripts were quantified using a
441 standard curve method. The ratio of interest (transcript/geometric) mean of two housekeeping

442 genes (RPLP0 and RPS17) was determined. The results were obtained from at least six
443 independent experiments, and all the steps followed the MIQE guidelines (Bustin *et al*, 2009).

444

445 **Western blot**

446 Primary amniocyte and AV3 cells were lysed in a RIPA buffer (20 mM Tris-HCl pH =
447 7.5, 150 mM NaCl, 1 % Nonidet P40, 0.5 % sodium deoxycholate, 1mM EDTA, 0.1 % SDS,
448 1x Complete Protease inhibitor cocktail (Roche) for 30 min at 4 °C. The amnion and
449 choriodecidua samples were homogenizated as described (Choltus *et al,* 2020). The protein
450 concentration of the supernatant was determined using a Pierce™ BCA Assay Kit (Pierce).
451 Forty µg of denaturated proteins were subjected to a Western blot analysis after 4–15 %
452 MiniPROTEAN® TGX StainFree™ gel electrophoresis (Bio-Rad) followed by probing
453 antibodies against TLR4 or β-Actin (TLR4:1:400, Sc-293072, Santa-Cruz Biotechnology, β-
454 Actin:1:10,000, MA1-91399, Thermo Fisher Scientific). The signal was detected with a
455 peroxidase-labeled anti-mouse antibody at 1:10,000 (Sc-2005, Santa Cruz Biotechnology) and
456 visualized with ECL or ECL2 Western blotting substrate (Pierce) using a ChemiDoc™ MP
457 Imaging System and Image Lab™ software (Bio-Rad). The results were obtained from at least
458 seven independent experiments and the relative TLR4 ratio was expressed in function of β-
459 Actin or total protein loaded by well.

460

461 **3'UTR-hTLR4 pMIR REPORT™ luciferase plasmid**

462 The 3'UTR hTLR4 (2,223 bp, NM 138554) was amplified from 100 ng of genomic
463 amnion DNA with 3'UTR-TLR4 primers containing Spe I restriction sites to facilitate
464 subcloning: forward GAGA*ACTAGT*AGAGGAAAAATAAAAACCTCCTG and reverse
465 GAGA *ACTAGT*TTGATATTATAAAACTGCATATATTTA. The PCR was performed with

466 Phusion® high-fidelity DNA polymerase (New England Biolabs) according to the
467 manufacturer's instructions. After purification and digestion with Spe I (New England Biolabs),
468 the fragment was subcloned into the Spe I site of the pMIR-REPORT™ luciferase vector
469 (Ambion, Thermo Fisher scientific) to generate the construct pMIR-3'UTR-hTLR4. The insert
470 sequence was checked by sequencing (Eurofins Genomics, Ebersberg, Germany).

471 ***In-silico* miRNA analysis**

472 Putative miRNAs targeting the 3'UTR-TLR4 target gene miRNA were screened using
473 the public database miRWalk with TargetScan, RNA22, and miRanda.

474

475 **Dual-Luciferase® Reporter assays**

476 HEK293 cells were cultured in six-well plates, transiently transfected at an 80–90 %
477 confluence using a Lipofectamine® 3000 Transfection Kit (Invitrogen, Thermo Fisher
478 Scientific). Each well received 100 ng of the pMIR-REPORT™ Luciferase vector containing
479 the 3'UTR-hTLR4 (without a negative control) in combination with 1µg pCMV-MIR or
480 pCMV-pre-mir125b1 (OriGene Technologies, Rockville, Maryland, USA) or let7A2 generated
481 in the laboratory and with 50 ng of pRL-TK Renilla luciferase plasmid (Promega).. Briefly, the
482 pre-let7A2 was amplified from 100 ng of genomic amnion DNA with pre-let7A2 primers
483 containing SgfI / MluI restriction sites to facilitate subcloning: forward
484 GAGA*GCGATCGC*TCGTCAACAGATATCAGAAGGC and reverse
485 GAGA*ACGCGT*AATGCTGCATTTTTTGTGACAATTT. The PCR was performed with
486 Advantage-HD DNA polymerase (Takara Bio, Saint-Germain-en-Laye, France) according to
487 the manufacturer's instructions. After purification and digestion with SgfI / MluI (New England
488 Biolabs), the fragment was subcloned into the SgfI / MluI site of the pCMV-MIR vector to

489 generate the construct pCMV-pre-let7A2. The insert sequence was checked by sequencing
490 (Eurofins Genomics, Ebersberg, Germany). Luciferase activity was measured using the Dual-
491 Luciferase® Reporter Assay System (Promega, Charbonnières-les-Bains, France) 48 h after
492 transfection according to the manufacturer's instructions using a Sirius luminometer (Berthold,
493 thoiry, France). Transfection efficiencies were normalized to the Renilla luciferase activities in
494 the corresponding wells and reported to the control condition. Data were extracted from at least
495 three experiments, each performed in triplicate.

496

497 **Transfections of primary amniocytes and AV3 cells**

498 Primary amniocytes and AV3 were cultured in six-well plates. At 80–90 % of
499 confluence, the cells were transiently transfected using a Lipofectamine® 3000 Transfection Kit
500 (Invitrogen, thermos Fisher Scientific) according to the protocol with 1µg expressing plasmid
501 of human pCMV pre-mir125b1, pre-let7A2, or a control (pCMV-MIR) purchased from
502 OriGene. After 48 h or 72 h of culturing, total RNA and proteins were respectively collected
503 and used for the qRT-PCR or Western blot experiments. Data were extracted from five
504 experiments.

505

506 **Statistical analysis**

507 The results were analyzed using PRISM software (GraphPad Software Inc., San Diego,
508 California, USA). The quantitative data were presented as the medians ± interquartile ranges
509 according to a Shapiro–Wilks test. Non-normally distributed data between the two groups were
510 studied with a Wilcoxon matched-pairs signed rank test for paired samples. To study several
511 independent groups, a Kruskal–Wallis test was performed followed by a Dunn's multiple

comparison test. Values were considered significantly different at $p < 0.05$ (*), $p < 0.01$ (**), or $p < 0.001$ (***) throughout.

ACKNOWLEDGEMENTS

LB was supported in carrying out this work by the Auvergne-Rhone-Alpes region's Jeune Chercheur framework. This research was conducted with the scientific support and expertise of Helixio (Saint-Beauzire, France).

AUTHOR CONTRIBUTIONS

CB, FPC, GC, MR, and CG conducted the experiments and acquired the data.

CB and BP conducted the statistical analyses.

DG, VS, and LB designed the research studies.

CB, VS, and LB wrote the manuscript.

CONFLICT OF INTEREST: The authors report no conflict of interest.

529 **DATA AVAILABILTY SECTION**

530 **-** Term W/O labor Fetal membrane methylation status results were submitted into Arrayexpress
531 (http://www.ebi.ac.uk/arrayexpress/experiments/E-MTAB-10520).

532 - Term W/O labor Fetal membrane mRNA expression results were submitted into Arrayexpress
533 (http://www.ebi.ac.uk/arrayexpress/experiments/E-MTAB-10516)

534

535 **REFERENCES**

536 Bustin SA, Benes V, Garson JA, Hellemans J, Huggett J, Kubista M, Mueller R, Nolan T, Pfaffl MW,
537 Shipley GL, *et al* (2009) The MIQE guidelines: minimum information for publication of
538 quantitative real-time PCR experiments. *Clin Chem* 55: 611–622

539 Chin PY, Dorian CL, Hutchinson MR, Olson DM, Rice KC, Moldenhauer LM & Robertson SA (2016)
540 Novel Toll-like receptor-4 antagonist (+)-naloxone protects mice from inflammation-induced
541 preterm birth. *Sci Rep* 6: 36112

542 Choi SJ, Jung S-H, Eom M, Han KH, Chung I-B & Kim S-K (2012) Immunohistochemical distribution of
543 toll-like receptor 4 in preterm human fetal membrane. *J Obstet Gynaecol Res* 38: 108–112

544 Choltus H, Lavergne M, Belville C, Gallot D, Minet-Quinard R, Durif J, Blanchon L & Sapin V (2020)
545 Occurrence of a RAGE-mediated inflammatory response in human fetal membranes. *Front*
546 *Physiol* 11

547 Cretoiu D, Xu J, Xiao J, Suciu N & Cretoiu SM (2016) Circulating MicroRNAs as potential molecular
548 biomarkers in the pathophysiological evolution of pregnancy. *Dis Markers* 2016: 3851054

549 Doridot L, Houry D, Gaillard H, Chelbi ST, Barbaux S & Vaiman D (2014) miR-34a expression,
550 epigenetic regulation, and function in human placental diseases. *Epigenetics* 9: 142–151

551 Eidem HR, Ackerman WE, McGary KL, Abbot P & Rokas A (2015) Gestational tissue transcriptomics in
552 term and preterm human pregnancies: a systematic review and meta-analysis. *BMC Med*
553 *Genomics* 8: 27

554 El Khwad M, Pandey V, Stetzer B, Mercer BM, Kumar D, Moore RM, Fox J, Redline RW, Mansour JM &
555 Moore JJ (2006) Fetal membranes from term vaginal deliveries have a zone of weakness
556 exhibiting characteristics of apoptosis and remodeling. *J Soc Gynecol Investig* 13: 191–195

557 Enquobahrie DA, Hensley M, Qiu C, Abetew DF, Hevner K, Tadesse MG & Williams MA (2016)
558 Candidate gene and MicroRNA expression in fetal membranes and preterm delivery risk.
559 *Reprod Sci Thousand Oaks Calif* 23: 731–737

560 Gillaux C, Méhats C, Vaiman D, Cabrol D & Breuiller-Fouché M (2011) Functional screening of TLRs in
561 human amniotic epithelial cells. *J Immunol* 187: 2766–2774

562 Goldenberg RL, Culhane JF, Iams JD & Romero R (2008) Epidemiology and causes of preterm birth.
563 *Lancet Lond Engl* 371: 75–84

564 Gomez-Lopez N, St. Louis D, Lehr MA, Sanchez-Rodriguez EN & Arenas-Hernandez M (2014) Immune
565 cells in term and preterm labor. *Cell Mol Immunol* 11: 571–581

566 Gonzalez JM, Xu H, Ofori E & Elovitz MA (2007) Toll-like receptors in the uterus, cervix, and placenta:
567 is pregnancy an immunosuppressed state? *Am J Obstet Gynecol* 197: 296.e1–6

568 Gu Y, Sun J, Groome LJ & Wang Y (2013) Differential miRNA expression profiles between the first and
569 third trimester human placentas. *Am J Physiol Endocrinol Metab* 304: E836-843

570 Haddad R, Tromp G, Kuivaniemi H, Chaiworapongsa T, Kim YM, Mazor M & Romero R (2006) Human
571 spontaneous labor without histologic chorioamnionitis is characterized by an acute
572 inflammation gene expression signature. *Am J Obstet Gynecol* 195: 394.e1–24

573 Han YM, Romero R, Kim J-S, Tarca AL, Kim SK, Draghici S, Kusanovic JP, Gotsch F, Mittal P, Hassan SS,
574 *et al* (2008) Region-specific gene expression profiling: novel evidence for biological
575 heterogeneity of the human amnion. *Biol Reprod* 79: 954–961

576 Harju K, Ojaniemi M, Rounioja S, Glumoff V, Paananen R, Vuolteenaho R & Hallman M (2005)
577 Expression of toll-like receptor 4 and endotoxin responsiveness in mice during perinatal
578 period. *Pediatr Res* 57: 644–648

579 Iliopoulos D, Hirsch HA & Struhl K (2009) An epigenetic switch involving NF-kappaB, Lin28, Let-7
580 MicroRNA, and IL6 links inflammation to cell transformation. *Cell* 139: 693–706

581 Joyce EM, Moore JJ & Sacks MS (2009) Biomechanics of the fetal membrane prior to mechanical
582 failure: review and implications. *Eur J Obstet Gynecol Reprod Biol* 144 Suppl 1: S121-127

583 Kamity R, Sharma S & Hanna N (2019) MicroRNA-mediated control of inflammation and tolerance in
584 pregnancy. *Front Immunol* 10: 718

585 Kawai T & Akira S (2010) The role of pattern-recognition receptors in innate immunity: update on
586 toll-like receptors. *Nat Immunol* 11: 373–384

587 Kendal-Wright CE (2007) Stretching, mechanotransduction, and proinflammatory cytokines in the
588 fetal membranes. *Reprod Sci Thousand Oaks Calif* 14: 35–41

589 Kim J, Pitlick MM, Christine PJ, Schaefer AR, Saleme C, Comas B, Cosentino V, Gadow E & Murray JC
590 (2013) Genome-wide analysis of DNA methylation in human amnion. *ScientificWorldJournal*
591 2013: 678156

592 Kim JK, Samaranayake M & Pradhan S (2009) Epigenetic mechanisms in mammals. *Cell Mol Life Sci*
593 *CMLS* 66: 596–612

594 Konwar C, Price EM, Wang LQ, Wilson SL, Terry J & Robinson WP (2018) DNA methylation profiling of
595 acute chorioamnionitis-associated placentas and fetal membranes: insights into epigenetic
596 variation in spontaneous preterm births. *Epigenetics Chromatin* 11

597 Krol J, Loedige I & Filipowicz W (2010) The widespread regulation of microRNA biogenesis, function
598 and decay. *Nat Rev Genet* 11: 597–610

599 Li L, Kang J & Lei W (2010) Role of Toll-like receptor 4 in inflammation-induced preterm delivery. *Mol*
600 *Hum Reprod* 16: 267–272

601 Li R, Ackerman WE, Summerfield TL, Yu L, Gulati P, Zhang J, Huang K, Romero R & Kniss DA (2011)
602 Inflammatory gene regulatory networks in amnion cells following cytokine stimulation:
603 translational systems approach to modeling human parturition. *PloS One* 6: e20560

604 Lim S, MacIntyre DA, Lee YS, Khanjani S, Terzidou V, Teoh TG & Bennett PR (2012) Nuclear factor
605 kappa B activation occurs in the amnion prior to labour onset and modulates the expression
606 of numerous labour associated genes. *PloS One* 7: e34707

607 Luo X, Shi Q, Gu Y, Pan J, Hua M, Liu M, Dong Z, Zhang M, Wang L, Gu Y, *et al* (2013) LncRNA pathway
608 involved in premature preterm rupture of membrane (PPROM): an epigenomic approach to
609 study the pathogenesis of reproductive disorders. *PloS One* 8: e79897

610 Marceau G, Gallot D, Borel V, Lémery D, Dastugue B, Dechelotte P & Sapin V (2006) Molecular and
611 metabolic retinoid pathways in human amniotic membranes. *Biochem Biophys Res Commun*
612 346: 1207–1216

613 Mauri A, Perrini M, Mateos JM, Maake C, Ochsenbein-Koelble N, Zimmermann R, Ehrbar M & Mazza
614 E (2013) Second harmonic generation microscopy of fetal membranes under deformation:
615 normal and altered morphology. *Placenta* 34: 1020–1026

616 McLaren J, Malak TM & Bell SC (1999) Structural characteristics of term human fetal membranes
617 prior to labour: identification of an area of altered morphology overlying the cervix. *Hum*
618 *Reprod Oxf Engl* 14: 237–241

619 McLaren J, Taylor DJ & Bell SC (2000) Increased concentration of pro-matrix metalloproteinase 9 in
620 term fetal membranes overlying the cervix before labor: implications for membrane
621 remodeling and rupture. *Am J Obstet Gynecol* 182: 409–416

622 McParland PC, Taylor DJ & Bell SC (2003) Mapping of zones of altered morphology and chorionic
623 connective tissue cellular phenotype in human fetal membranes (amniochorion and decidua)
624 overlying the lower uterine pole and cervix before labor at term. *Am J Obstet Gynecol* 189:
625 1481–1488

626 Medzhitov R, Preston-Hurlburt P & Janeway CA (1997) A human homologue of the Drosophila Toll
627 protein signals activation of adaptive immunity. *Nature* 388: 394–397

628 Metropolis N & Ulam S (1949) The Monte Carlo method. *J Am Stat Assoc* 44: 335–341

629 Moço NP, Martin LF, Pereira AC, Polettini J, Peraçoli JC, Coelho KIR & da Silva MG (2013) Gene
630 expression and protein localization of TLR-1, -2, -4 and -6 in amniochorion membranes of
631 pregnancies complicated by histologic chorioamnionitis. *Eur J Obstet Gynecol Reprod Biol*
632 171: 12–17

633 Montenegro D, Romero R, Kim SS, Tarca AL, Draghici S, Kusanovic JP, Kim JS, Lee DC, Erez O, Gotsch
634 F, *et al* (2009) Expression patterns of microRNAs in the chorioamniotic membranes: a role for
635 microRNAs in human pregnancy and parturition. *J Pathol* 217: 113–121

636 Montenegro D, Romero R, Pineles BL, Tarca AL, Kim YM, Draghici S, Kusanovic JP, Kim J-S, Erez O,
637 Mazaki-Tovi S, *et al* (2007) Differential expression of microRNAs with progression of
638 gestation and inflammation in the human chorioamniotic membranes. *Am J Obstet Gynecol*
639 197: 289.e1–6

640 Morales-Prieto DM, Ospina-Prieto S, Chaiwangyen W, Schoenleben M & Markert UR (2013)
641 Pregnancy-associated miRNA-clusters. *J Reprod Immunol* 97: 51–61

642 Musilova I, Kutová R, Pliskova L, Stepan M, Menon R, Jacobsson B & Kacerovsky M (2015)
643 Intraamniotic inflammation in women with preterm pre-labor rupture of membranes. *PloS*
644 *One* 10: e0133929

645 Newton K & Dixit VM (2012) Signaling in innate immunity and inflammation. *Cold Spring Harb*
646 *Perspect Biol* 4

647 Nhan-Chang C-L, Romero R, Tarca AL, Mittal P, Kusanovic JP, Erez O, Mazaki-Tovi S, Chaiworapongsa
648 T, Hotra J, Than NG, *et al* (2010) Characterization of the transcriptome of chorioamniotic

649 membranes at the site of rupture in spontaneous labor at term. *Am J Obstet Gynecol* 202:
650 462.e1–41

651 Nyholm AM, Lerche CM, Manfé V, Biskup E, Johansen P, Morling N, Thomsen BM, Glud M &
652 Gniadecki R (2014) miR-125b induces cellular senescence in malignant melanoma. *BMC*
653 *Dermatol* 14: 8

654 Osman I, Young A, Jordan F, Greer IA & Norman JE (2006) Leukocyte density and proinflammatory
655 mediator expression in regional human fetal membranes and decidua before and during
656 labor at term. *J Soc Gynecol Investig* 13: 97–103

657 Patni S, Flynn P, Wynen LP, Seager AL, Morgan G, White JO & Thornton CA (2007) An introduction to
658 toll-like receptors and their possible role in the initiation of labour. *BJOG Int J Obstet*
659 *Gynaecol* 114: 1326–1334

660 Poltorak A, He X, Smirnova I, Liu MY, Van Huffel C, Du X, Birdwell D, Alejos E, Silva M, Galanos C, *et al*
661 (1998) Defective LPS signaling in C3H/HeJ and C57BL/10ScCr mice: mutations in Tlr4 gene.
662 *Science* 282: 2085–2088

663 Prat C, Bouvier D, Comptour A, Marceau G, Belville C, Clairefond G, Blanc P, Gallot D, Blanchon L &
664 Sapin V (2015) All-trans-retinoic acid regulates aquaporin-3 expression and related cellular
665 membrane permeability in the human amniotic environment. *Placenta* 36: 881–887

666 Robertson SA, Hutchinson MR, Rice KC, Chin P-Y, Moldenhauer LM, Stark MJ, Olson DM & Keelan JA
667 (2020) Targeting Toll-like receptor-4 to tackle preterm birth and fetal inflammatory injury.
668 *Clin Transl Immunol* 9: e1121

669 Romero R, Espinoza J, Gonçalves LF, Kusanovic JP, Friel LA & Nien JK (2006a) Inflammation in preterm
670 and term labour and delivery. *Semin Fetal Neonatal Med* 11: 317–326

671 Romero R, Espinoza J, Kusanovic JP, Gotsch F, Hassan S, Erez O, Chaiworapongsa T & Mazor M
672 (2006b) The preterm parturition syndrome. *BJOG Int J Obstet Gynaecol* 113 Suppl 3: 17–42

673 Roush S & Slack FJ (2008) The let-7 family of microRNAs. *Trends Cell Biol* 18: 505–516

674 Schulte LN, Eulalio A, Mollenkopf H-J, Reinhardt R & Vogel J (2011) Analysis of the host microRNA
675 response to Salmonella uncovers the control of major cytokines by the let-7 family. *EMBO J*
676 30: 1977–1989

677 Silva M de C, Richardson LS, Kechichian T, Urrabaz-Garza R, Silva MG da & Menon R (2020)
678 Inflammation, but not infection, induces EMT in human amnion epithelial cells. *Reproduction*
679 160: 627–638

680 Stephen GL, Lui S, Hamilton SA, Tower CL, Harris LK, Stevens A & Jones RL (2015) Transcriptomic
681 profiling of human choriodecidua during term labor: inflammation as a key driver of labor.
682 *Am J Reprod Immunol N Y N 1989* 73: 36–55

683 Supek F, Bošnjak M, Škunca N & Šmuc T (2011) REVIGO summarizes and visualizes long lists of gene
684 ontology terms. *PloS One* 6: e21800

685 Tili E, Michaille J-J, Cimino A, Costinean S, Dumitru CD, Adair B, Fabbri M, Alder H, Liu CG, Calin GA, *et*
686 *al* (2007) Modulation of miR-155 and miR-125b levels following lipopolysaccharide/TNF-

687 alpha stimulation and their possible roles in regulating the response to endotoxin shock. *J*
688 *Immunol Baltim Md 1950* 179: 5082–5089

689 Wahid HH, Dorian CL, Chin PY, Hutchinson MR, Rice KC, Olson DM, Moldenhauer LM & Robertson SA
690 (2015) Toll-like receptor 4 is an essential upstream regulator of on-time parturition and
691 perinatal viability in mice. *Endocrinology* 156: 3828–3841

692 Wang H & Hirsch E (2003) Bacterially-induced preterm labor and regulation of prostaglandin-
693 metabolizing enzyme expression in mice: the role of toll-like receptor 4. *Biol Reprod* 69:
694 1957–1963

695 Wang H, Ogawa M, Wood JR, Bartolomei MS, Sammel MD, Kusanovic JP, Walsh SW, Romero R &
696 Strauss JF (2008) Genetic and epigenetic mechanisms combine to control MMP1 expression
697 and its association with preterm premature rupture of membranes. *Hum Mol Genet* 17:
698 1087–1096

699 Wang Y, Lv Y, Gao S, Zhang Y, Sun J, Gong C, Chen X & Li G (2016) MicroRNA profiles in spontaneous
700 decidualized menstrual endometrium and early pregnancy decidua with successfully
701 implanted embryos. *PloS One* 11: e0143116

702 Waters TP & Mercer B (2011) Preterm PROM: prediction, prevention, principles. *Clin Obstet Gynecol*
703 54: 307–312

704 Yoo JY, You Y-A, Kwon EJ, Park MH, Shim S & Kim YJ (2018) Differential expression and methylation of
705 integrin subunit alpha 11 and thrombospondin in the amnion of preterm birth. *Obstet*
706 *Gynecol Sci* 61: 565

707

708

709 **FIGURE LEGENDS**

710

711 **Figure 1: Differential cytosine methylation is analyzed for the ZIM and the ZAM.**

712 A Genes affected by differential methylation between the amnion and the choriodecidua,
713 separately studied for the ZIM (left) and the ZAM (right).

714 B Four-way Venn diagram representing the number of genes with hypermethylated cytosines
715 in the ZIM and the ZAM according to the methylomic analyses. mA > mC: a specific gene
716 was more methylated in the amnion than in the choriodecidua. mA < mC: a specific gene
717 was less methylated in the amnion than in the choriodecidua.

718 C GO-term classifications for genes observed specifically in the ZAM: mA > mC (left panel)
719 and mA < mC (right panel). A Bonferroni correction was conducted for p-values < 0.01.

720

721 **Figure 2: Transcriptomic assay is analyzed for the ZAM in fetal membranes.**

722 A Volcano plots represent the log10 adjusted p-values versus the log2 fold change (FC). Up-
723 and downregulated genes are shown in red and blue, respectively, limited by $|\log_2 FC| = 2.8$.
724 They are classified in a four-way-Venn diagram representing the gene numbers in the ZIM
725 and ZAM analyses with $|\log_2 FC| = 2.8$.

726 B GO-term classifications are shown for genes expressed only in the ZAM for log2 FC < 2.8
727 (Bonferroni correction for p-values < 0.01)

728 C GO-term classifications are shown for genes expressed only in the ZAM for log2 FC > 2.8
729 (uncorrected p-value < 0.01).

730

731 **Figure 3: Common genes are observed between the mA > mC methylomic results and the**
732 **choriodecidua/amnion transcriptomic analysis in the ZAM.**

733 A GO terms' representative distribution and their log10 p-values are shown for the 105 common
734 genes across both genome-wide studies.
735 B Representative TLR4 immunofluorescence (green staining) in the ZAM of fetal membranes
736 in the confocal analyses. Cell nuclei were visualized with Hoescht (blue) staining. A negative
737 control was used without a primary antibody. Slides were observed at x250 magnification
738 for total fetal membranes (left and right): scale bar: 50µm and x400 for the amnion (middle):
739 scale bar: 20µm.
740 C Luminex technology was used to detect physiological IL-6 and TNF-α levels and to
741 demonstrate no (or a weak) presence of this interleukin in the amnion or the choriodecidua
742 (NT condition). After treatment for 24 h with LPS (0.5µg/ml), the levels of IL-6 (n=6) and
743 TNF-α (n=6) significantly increased. Median ± interquartile ranges are represented
744 (Wilcoxon matched-pairs signed rank test, * p-value < 0.05).
745
746 **Figure 4: The expression level of the TLR4 gene is related to its cytosine methylation level**
747 **in the amnion and the choriodecidua.**
748 A Top: The median ± interquartile ranges of the DNA methylation levels of the five cg probes
749 on the TLR4 gene in the amnion and choriodecidua ZAMs. Each dot represents the
750 individual β-value for one patient (n=9). The probe set with significant differential
751 methylation between the amnion and choriodecidua (Wilcoxon matched-pairs signed rank
752 test) is designated by an asterisk (** p-value < 0.01). Bottom: Control of the difference of
753 methylation for the cg 05429895 between the amnion and the choriodecidua after digestion
754 with Taq I PCR products (438 bp) obtained after DNA bisulfite treatment. This probe,
755 methylated in the amnion, was sensitive to Taq I and gave two fragments after digestion:
756 307 bp and 131 bp.

757 B Relative expression of TLR4 transcripts for the nine samples of choriodecidua ZAM were
758 significantly higher than for the amnion ZAM (Wilcoxon matched-pairs signed rank test *
759 p-value < 0.05).
760 C The TLR4 protein was significantly overexpressed for the nine samples in the choriodecidua
761 compared to the amnion (Wilcoxon matched-pairs signed rank test * p-value < 0.05).
762

763 **Figure 5: Two miRNAs potentially targeting the human 3'UTR-TLR4 are differentially**
764 **methylated in the ZAM between the amnion and the choriodecidua.**
765 A *In-silico* computational target prediction analysis using TargetScan of the human 3'UTR-
766 TLR4. This zone may be targeted by gene coding for MIR125B1 and LET7A2.
767 B The median ± interquartile ranges of the DNA methylation cg probe levels for the MIR125B1
768 (top) and LET7A2 (bottom) genes for the nine samples in the amnion and choriodecidua
769 ZAM. Each dot represents the individual β-value for one patient. The probe set with
770 significant differential methylation between the amnion and choriodecidua (Wilcoxon
771 matched-pairs signed rank test) is designated by an asterisk (** p-value < 0.01, NS = not
772 significant).
773 C The relative expression of pri-miR-125b-1 (n=9) and pri-let-7a-2 (n=5) was determined. qRT-
774 PCR experiments performed for each zone, and tissue demonstrated that pri-miR-125b-1
775 was significantly overexpressed in the amnion compared to the choriodecidua ZAM, as
776 expected from the differential methylation status (Wilcoxon matched-pairs signed rank test
777 * p-value < 0.05). The pri-let-7a-2 amount could not be rigorously determined (ND) in the
778 choriodecidua.

779

780 **Figure 6: miR-125b-1 and let-7a-2 target the human 3'UTR-TLR4 and decrease TLR4**
781 **expression**

782 A Targeting of miR-125b-1 and let-7a-2 to the human 3'UTR of TLR4 mRNA using a
783 Luciferase Reporter Gene Assay depending on human 3'UTR-TLR4 (pMIR-3'UTR TLR4-
784 luc). HEK293 cells co-transfected for 48 h with this construction and expressing plasmid
785 of human pCMV, pre-mir125b1, or let7A2 (n=5). Luciferase activity was normalized with
786 the pRL-TK- Renilla-luciferase level (median ± interquartile range, Kruskal-Wallis test
787 with Dunn's multiple comparison test, * p-value < 0.05). The results showed that both
788 miRNAs were able to target the 3'-UTR zone of the TLR4 gene and to decrease luciferase
789 quantity.
790 B Determination of endogenous TLR4 expression levels in human cell lines (HEK293 from
791 embryonic kidney, and FL, WISH, and AV3 from Amniocytes) and in primary Amniocyte
792 cells quantified by qRT-PCR (n=6).
793 C Effects of miR-125b-1, let-7a-2, and the combination miR-125b-1 + let-7a-2 on TLR4 mRNA
794 expression (n=10 for 12h and n=8 for 24h, left) and TLR4 protein (n=7, right) in AV3 cells.
795 Cells were transfected with expressing plasmid of human pCMV, or pre-mir125b1, or
796 let7A2 and miR-125b-1 + let-7a-2 for 12 h and 24 h for mRNA, and 24 h and 48 h for
797 protein (median ± interquartile range, Kruskal-Wallis test with Dunn's multiple
798 comparison test, * p-value < 0.05, ** p-value < 0.01).
799 D Effects of miR-125b-1, let-7a-2, and the combination miR-125b-1 + let-7a-2 on TLR4
800 mRNA expression (n=7 at least, left) at 48 h and TLR4 protein (n=5 at least, right) at 72 h
801 in primary Amniocyte cells (median ± interquartile ranges, Kruskal-Wallis test with
802 Dunn's multiple comparison test, * p-value < 0.05, ** p-value < 0.01, *** p-value<0.001).
803

804 **Figure 7: A model for the regulation of TLR4 expression in human fetal membranes is**
805 **proposed.**
806

807 **ADDITIONAL FILES**

808 **SUPPLEMENTARY TABLES:**

809 **Table S1: Perinatal characteristics of the enrolled patients.**

810 F = Female, M = Male. Data are expressed as the mean ± SEM.

811 **Table S2: Primer sequences used for the PCR.**

812 **Table S3**: List of specific genes extracted from the ZAM zone after a transcriptomic analysis.

813 **Table S4:** List of jointly hypermethylated genes in the ZAM choriodecidua and overexpressed
814 in the ZAM amnion.

815 **Table S5:** List of disease mesh-terms associated with hypermethylated genes in the ZAM
816 choriodecidua and overexpressed in the ZAM Amnion.

817 **Table S6:** List of jointly hypermethylated genes in the ZAM amnion and overexpressed in the
818 ZAM choriodecidua.

819 **Table S7:** List of disease mesh-terms associated with hypermethylated genes in the ZAM
820 amnion and overexpressed in the ZAM choriodecidua**.**

821

822 **TRANSPARENT REPORTING FORM**

823

824 **FIGURES SOURCE DATA:**

825 **Figure 3-source data 1:** Raw data for TLR4 immunofluorescence in the fetal membranes by
826 confocal microscopy.

827 **Figure 3-source data 2:** Data on IL-6 and TNF-α concentrations in amnion and
828 choriodecidua.

829 **Figure 4-source data 1:** Data on β-value for cg probes on the TLR4 gene for Figure 4A.

830 **Figure 4-source data 2:** Uncropped polyacrylamide gel for Figure 4B.

831 **Figure 4-source data 3:** qRT-PCR data and Western-blots data for TLR4 expression (Figure
832 4C).

833 **Figure 5-source data 1:** Data on β-value for cg probes on the MIR125B1 and LET7A2 genes
834 for Figure 5B.

835 **Figure 5-source data 2:** qRT-PCR data for pri-miR-125b-1 and pri-let-7a-2 (Figure 5C).

836 **Figure 6-source data 1:** Data on luciferase activity in HEK293 cells transfected with pMIR-
837 3'UTR TLR4-luc and pre-mir125b1 or let7A2 (Figure 6A)

838 **Figure 6-source data 2:** qRT-PCR data for TLR4 expression for Figure 6B.

839 **Figure 6-source data 3:** qRT-PCR data and Western-blots data for TLR4 expression in AV3
840 cells transfected with pre-miRNA (Figure 6C).

841 **Figure 6-source data 4:** qRT-PCR data and Western-blots data for TLR4 expression in
842 Amniocytes transfected with pre-miRNA (Figure 6D).

A

	ZIM		ZAM	
	Hypermethylated Cytosines in Amnion (mA)	Hypermethylated Cytosines in Choriodecidua (mC)	Hypermethylated Cytosines in Amnion (mA)	Hypermethylated Cytosines in Choriodecidua (mC)
Genes Number	322	1424	5086	4744

B

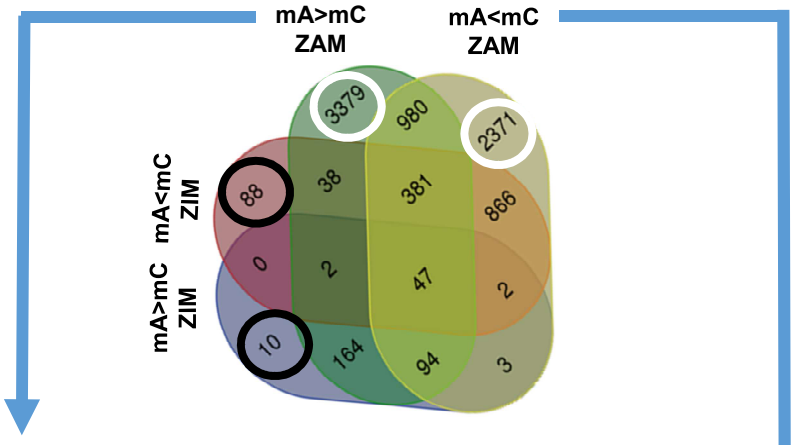

C

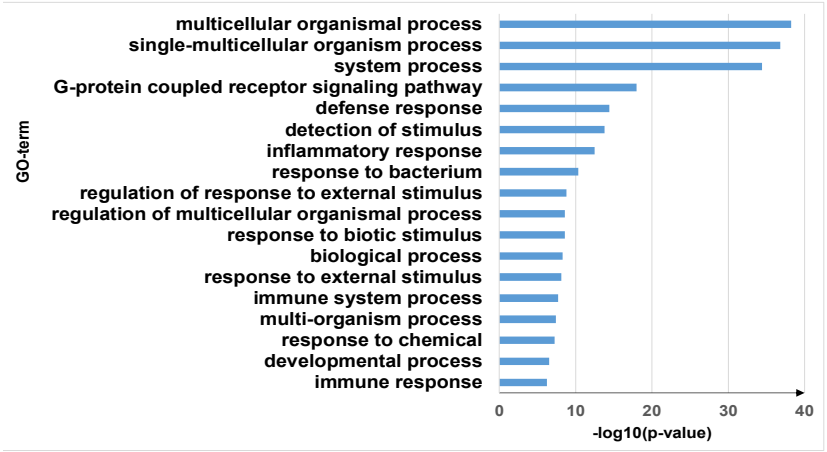

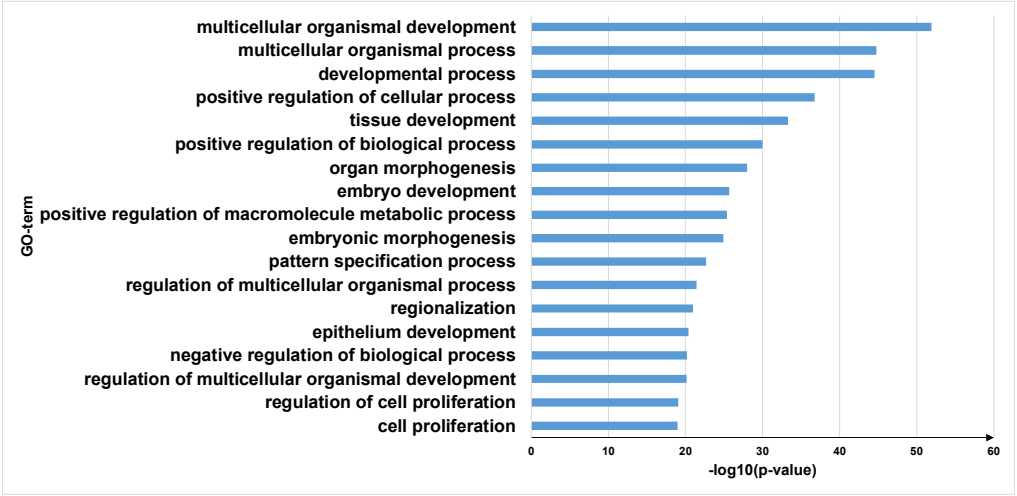

Figure 1

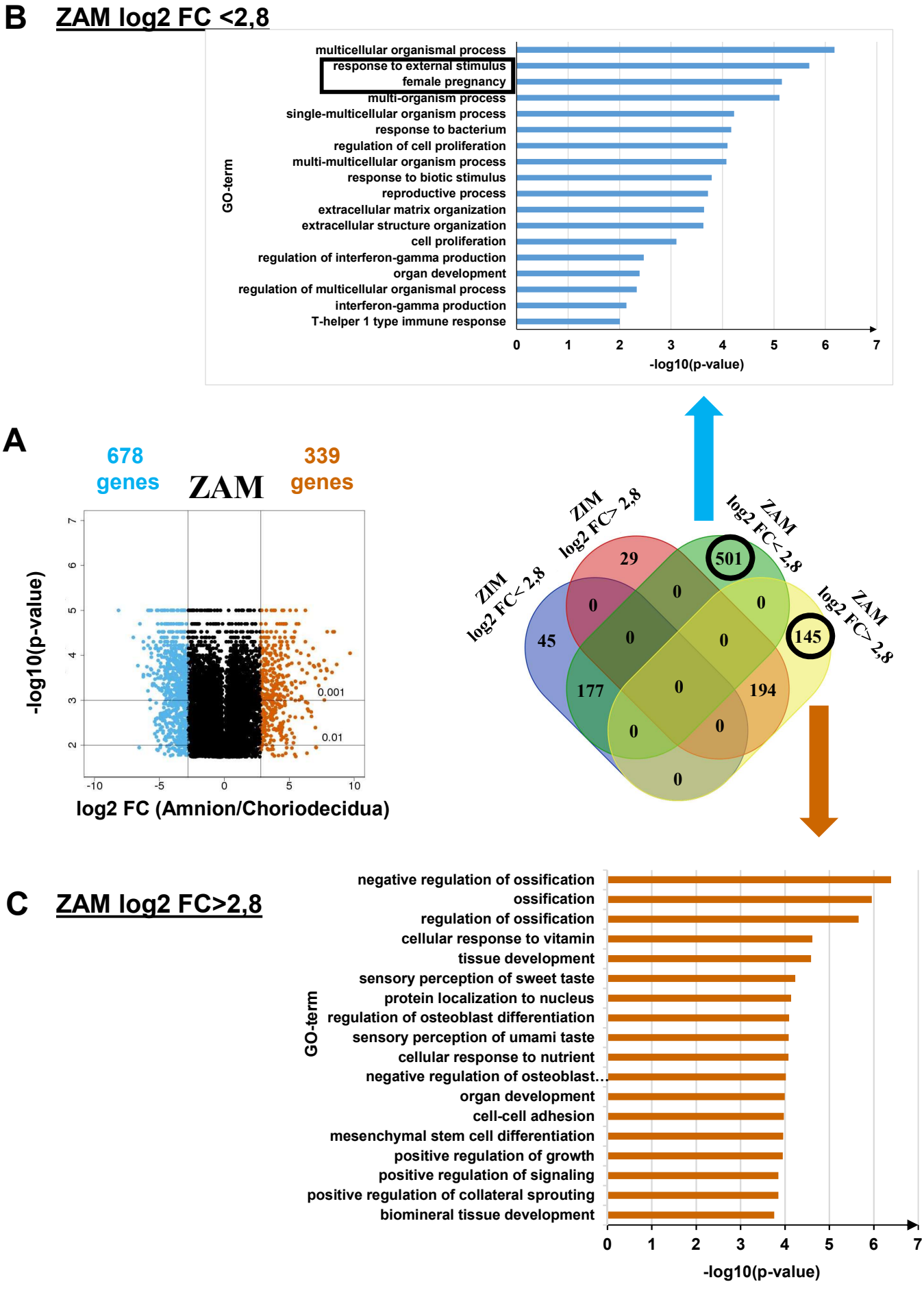
B
ZAM log2 FC <2,8
multicellular organismal process
response to external stimulus
female pregnancy
multi-organism process
single-multicellular organism process
response to bacterium
regulation of cell proliferation
multi-multicellular organism process
response to biotic stimulus
reproductive process
extracellular matrix organization
extracellular structure organization
cell proliferation
regulation of interferon-gamma production
organ development
regulation of multicellular organismal process
interferon-gamma production
T-helper 1 type immune response
GO-term
0 1 2 3 4 5 6 7
-log10(p-value)
A
678 genes
ZAM
339 genes
-log10(p-value)
0.001
0.01
-10 -5 0 5 10
log2 FC (Amnion/Choriodecidua)
ZIM log2 FC< 2,8
ZIM log2 FC> 2,8
ZAM log2 FC< 2,8
ZAM log2 FC> 2,8
45
29
501
145
0
177
194
C
ZAM log2 FC>2,8
negative regulation of ossification
ossification
regulation of ossification
cellular response to vitamin
tissue development
sensory perception of sweet taste
protein localization to nucleus
regulation of osteoblast differentiation
sensory perception of umami taste
cellular response to nutrient
negative regulation of osteoblast...
organ development
cell-cell adhesion
mesenchymal stem cell differentiation
positive regulation of growth
positive regulation of signaling
positive regulation of collateral sprouting
biomineral tissue development
GO-term
0 1 2 3 4 5 6 7
-log10(p-value)

Figure 2

A

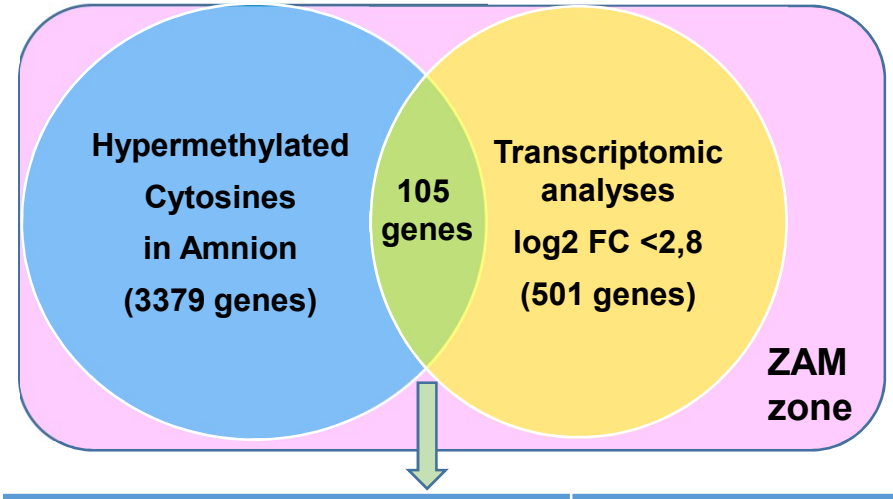

GO-term	-log10(p-value)
Extracellular structure organization	6,93
Response to external stimulus	5,07
Detection of lipopolysaccharide	3,8
Inflammatory response	3,29

B

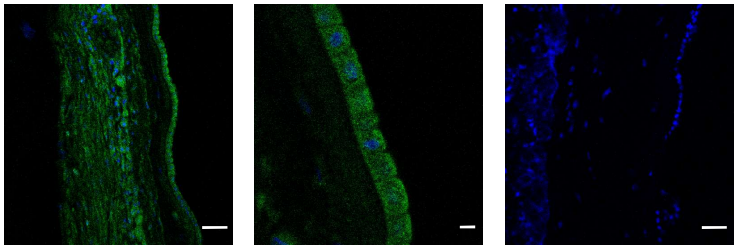

Fetal membranes | Amnion | Negative Control

C

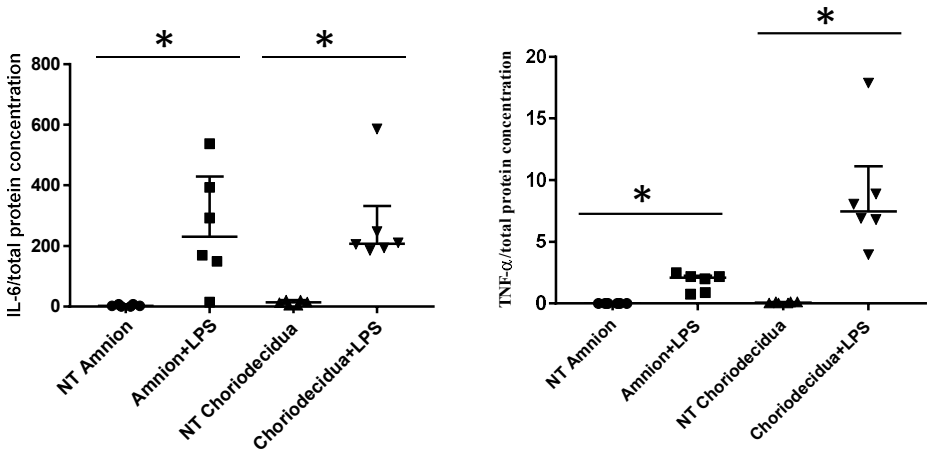

Figure 3

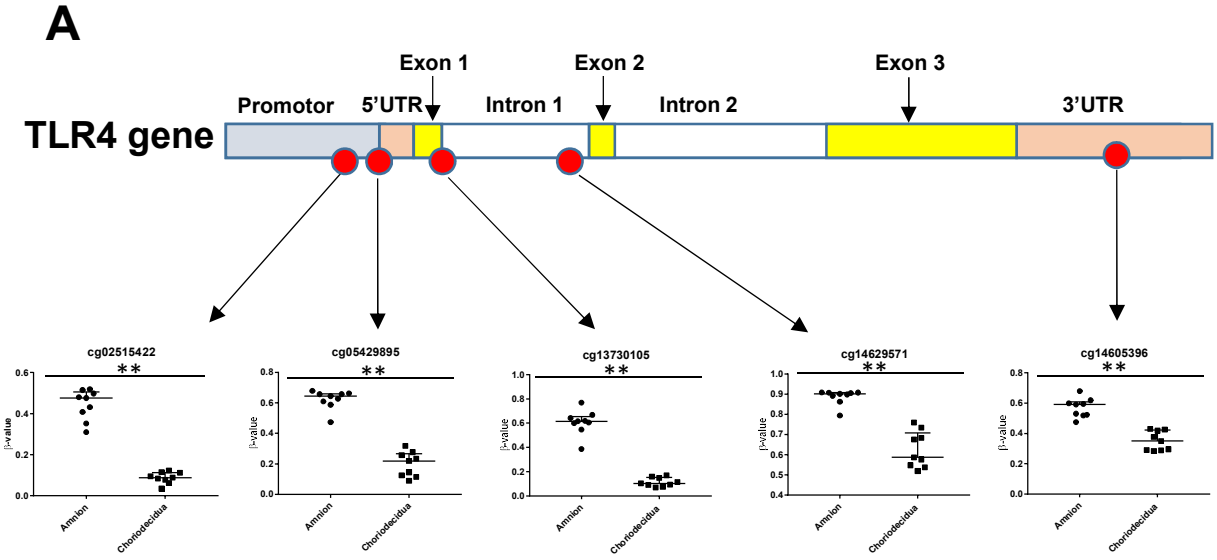
A
TLR4 gene
Promotor
5'UTR
Exon 1
Intron 1
Exon 2
Intron 2
Exon 3
3'UTR
cg02515422
cg05429895
cg13730105
cg14629571
cg14605396
β-value
Amnion
Choriodecidua

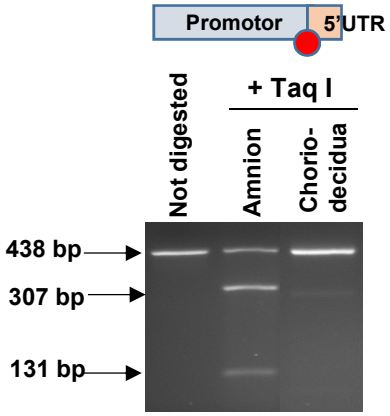
B
Promotor
5'UTR
+ Taq I
Not digested
Amnion
Chorio-decidua
438 bp
307 bp
131 bp

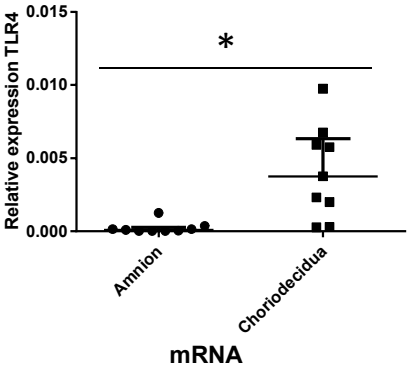
C
Relative expression TLR4
0.015
0.010
0.005
0.000
*
Amnion
Choriodecidua
mRNA

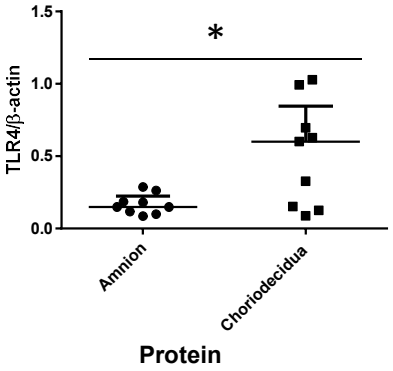
D
TLR4/β-actin
1.5
1.0
0.5
0.0
*
Amnion
Choriodecidua
Protein

Figure 4

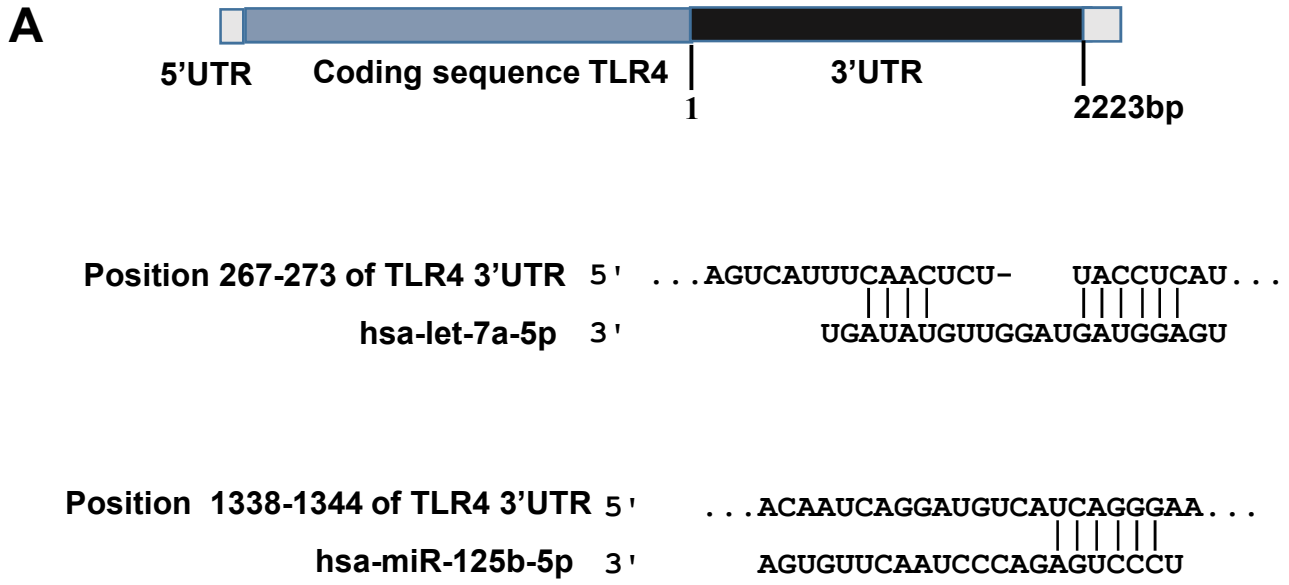
A
5'UTR
Coding sequence TLR4
3'UTR
1
2223bp
Position 267-273 of TLR4 3'UTR 5' ...AGUCAUUUCAACUCU- UACCUCAU...
hsa-let-7a-5p 3' UGAUAUGUUGGAUGAUGGAGU
Position 1338-1344 of TLR4 3'UTR 5' ...ACAAUCAGGAUGUCAUCAGGGAA...
hsa-miR-125b-5p 3' AGUGUUCAAUCCCAGAGUCCCU

Figure 5

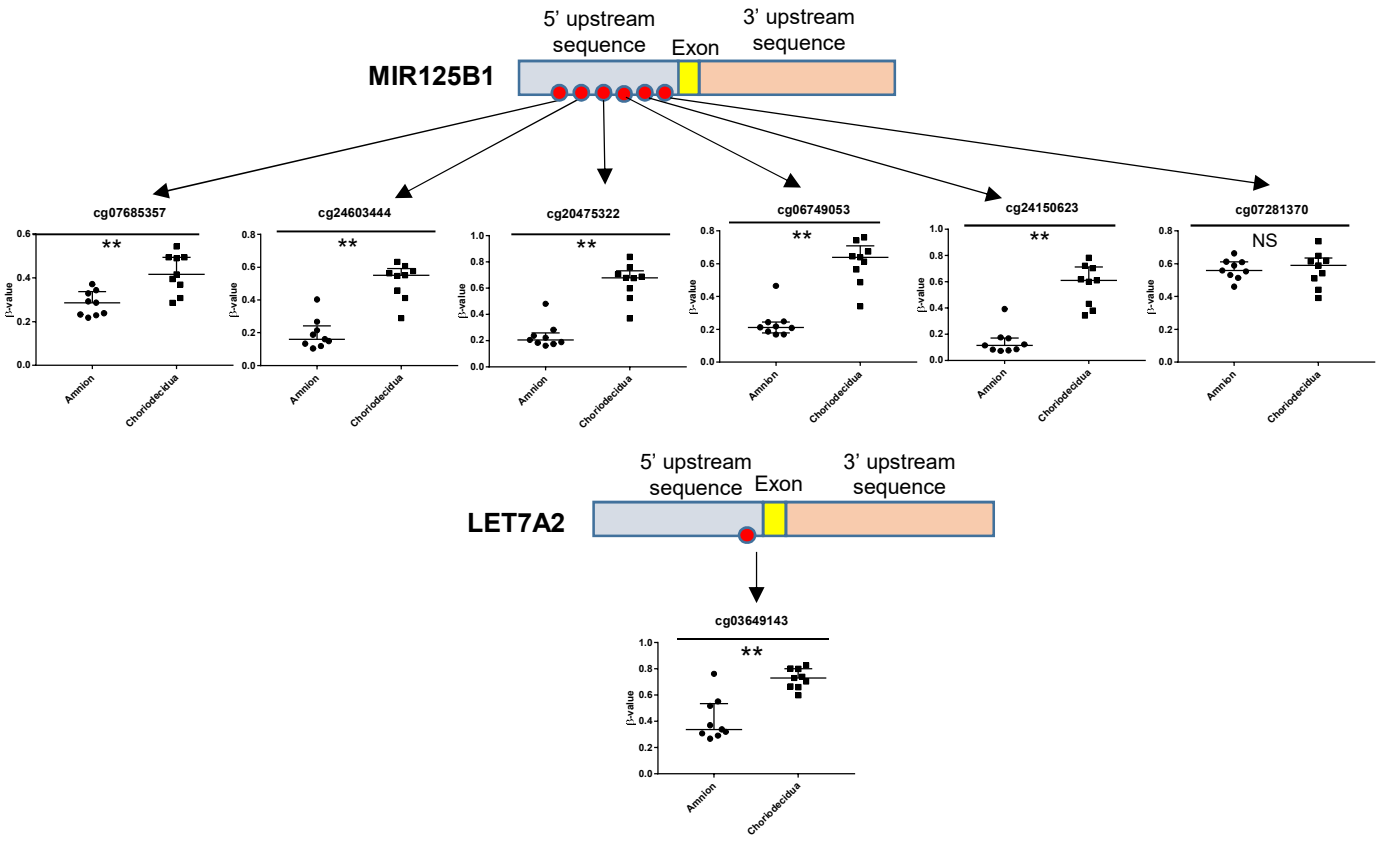
B
5' upstream sequence
Exon
3' upstream sequence
MIR125B1
cg07685357
cg24603444
cg20475322
cg06749053
cg24150623
cg07281370
NS
β-value
Amnion
Choriodecidua
LET7A2
cg03649143

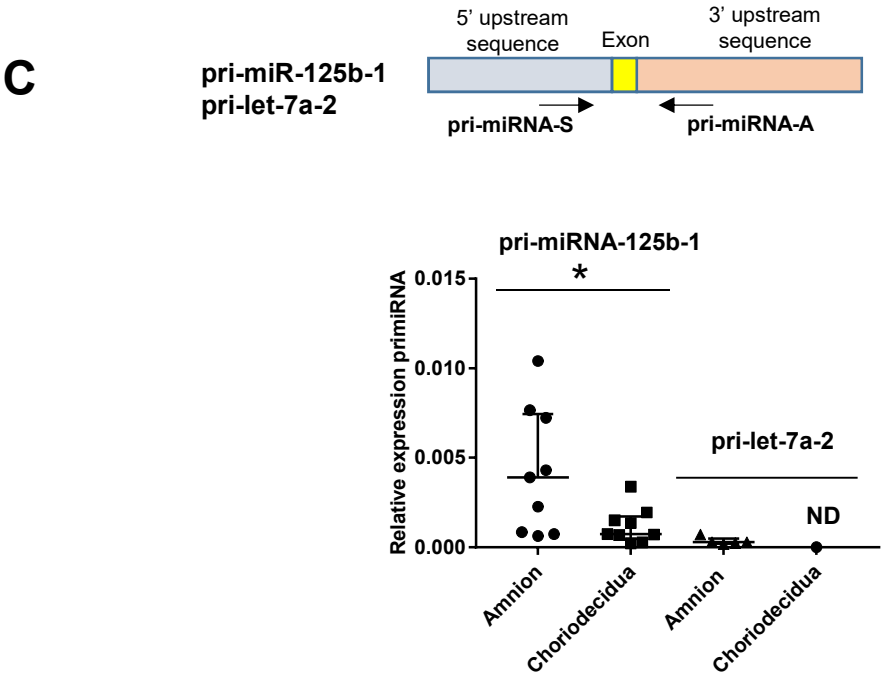
C
pri-miR-125b-1
pri-let-7a-2
5' upstream sequence
Exon
3' upstream sequence
pri-miRNA-S
pri-miRNA-A
pri-miRNA-125b-1
pri-let-7a-2
ND
Relative expression primiRNA
0.015
0.010
0.005
0.000
Amnion
Choriodecidua

Figure 5

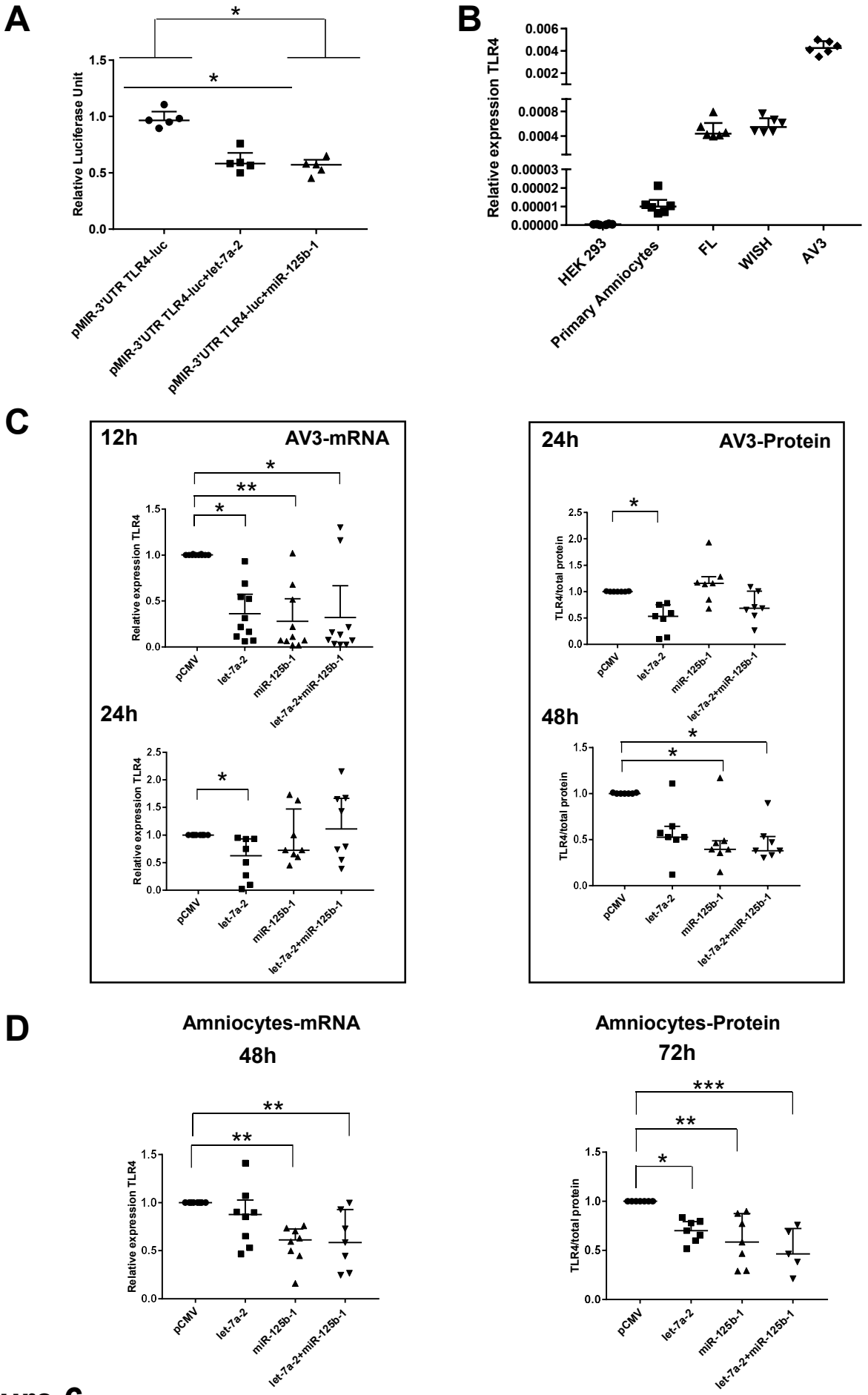
A
Relative Luciferase Unit
pMIR-3'UTR TLR4-luc
pMIR-3'UTR TLR4-luc+let-7a-2
pMIR-3'UTR TLR4-luc+miR-125b-1
B
Relative expression TLR4
HEK 293
Primary Amniocytes
FL
WISH
AV3
C
12h
AV3-mRNA
24h
AV3-Protein
48h
Relative expression TLR4
TLR4/total protein
pCMV
let-7a-2
miR-125b-1
let-7a-2+miR-125b-1
D
Amniocytes-mRNA
48h
Amniocytes-Protein
72h

Figure 6

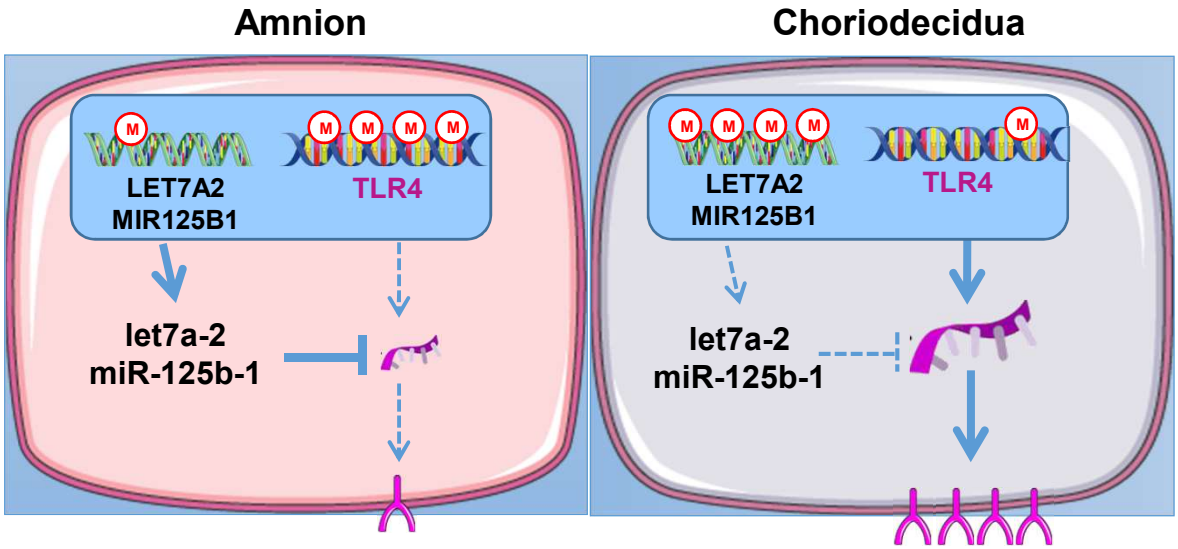
Amnion
Choriodecidua
M
LET7A2
MIR125B1
TLR4
let7a-2
miR-125b-1

Figure 7

Key resources table

Reagent type (species) or resource	Designation
Antibody	Monoclonal mouse anti-TLR4
Antibody	Monoclonal mouse anti-β Actin
Cell line	Human epithelial amnion cells AV3
Cell line	Human epithelial amnion cells FL
Cell line	Human epithelial amnion cells WISH
Cell line	Human embryonic kidney (HEK) 293
Commercial assay or kit	QIAamp® DNA Mini Kit
Commercial assay or kit	EZ DNA Methylation™ Kit
Commercial assay or kit	Bio-Plex Pro™ Human Cytokine 27-plex Assay
Commercial assay or kit	BCA Assay kit
Commercial assay or kit	RNeasy® Mini Kit
Commercial assay or kit	SuperScript™ III First-Strand Synthesis System
Commercial assay or kit	Dual-Luciferase® Reporter Assay System
Commercial assay or kit	Lipofectamine® 3000 Transfection Kit
Software, algorithm	GraphPad Prism Software
Software, algorithm	GePS Genomatix
Software, algorithm	Image Lab™ software
Software, algorithm	miRWalk
Software, algorithm	R (CRAN)
Software, algorithm	Generic GO term finder

Software, algorithm	Bioconductor
Software, algorithm	REVIGO
Chemical compound, drug	LPS from E.coli (O55:B5)
Recombinant DNA reagent	pMIR-REPORT™ luciferase vector
Recombinant DNA reagent	pCMV-MIR
Recombinant DNA reagent	pCMV-pre-mir125b1
Recombinant DNA reagent	pCMV-pre-let7A2
Recombinant DNA reagent	pRL-TK Renilla luciferase plasmid

Source or reference	Identifiers	Additional information
Santa-Cruz Biotechnologies	Sc-293072, RRID:AB_10611320	IF (1:400), WB (1:400)
ThermoFisher Scientific	MA1-91399,	WB (1:10000)
ATCC	CCL-21, RRID:CVCL_1904	
ATCC	CCL-62, RRID:CVCL_1905	
ATCC	CCL-25, RRID:CVCL_1909	
ATCC	CRL-1573, RRID:CVCL_0045	
Qiagen	Cat #: 51306	
Zymo research	Cat #: D5005	
Bio-Rad	Cat #: M500KCAF0Y	
Pierce	Cat #: 23227	
Qiagen	Cat #:74106	
Invitrogen	Cat #: 18080051	
Promega	Cat #:E1910	
Invitrogen	Cat #: L3000001	
GraphPad	RRID:SCR_002798	
Genomatix	RRID:SCR_008036	
Bio-Rad	RRID:SCR_014210	
http://mirwalk.umm.uni-heidelberg.de/	RRID:SCR_016509	
https://cran.r-project.org/	RRID:SCR_003005	
http://go.princeton.edu	RRID:SCR_008870	

https://bioconductor.org/	RRID #:SCR_006442	
http://revigo.irb.hr/	RRID:SCR_005825	
Sigma-Aldrich Chimie	L2880	0,5µg/ml
Ambion	Cat #: AM5795	
OriGene Technologies	Cat #: PCMVMIR	
OriGene Technologies	Cat #: SC400083	
OriGene Technologies	Generated in this paper	
Promega	Cat #: E2241	

Table S1 :

Perinatal characteristics of the enrolled patients.

Perinatal characteristics	n=9
Maternal Age (years)	32.33 ± 1.76
Gestational age at delivery (Amenorrhea weeks)	39.10 ± 0.08
Body Mass Index, BMI	23.75 ± 0.95
Child sexe	5F, 4M
Birth weight (g)	3351 ± 129

Table S2:

Primer sequences used for the PCR.

Human Gene	Sequence (5'→3')	Product length (bp)	NCBI Reference
hTLR4-S	ACCAAGAACCTGGACCTGAG	181	NM_138554
hTLR4-A	TCTGGATGGGGTTTCCTGTC		
hRPLP0-S	AGGCTTTAGGTATCACCACT	219	NM_053275
hRPLP0-A	GCAGAGTTTCCTCTGTGATA		
hRPS17-S	TGCGAGGAGATCGCCATTATC	170	NM_001021
hRPS17-A	AAGGCTGAGACCTCAGGAAC		
hpri-125B1-S	CGAACAGAAATTGCCTGTCATTC	175	NR_029671
hpri-125B1-A	TTCCACCAAATTTCCAGGATGC		
hpri-LET7A2-S	AGACTAACTTGTAATTTCCCTGC	190	NR_029477
hpri-LET7A2-A	AGGCCTGGAGGAATCATGATC		
hpri-LET7A1-S	TTCCTGTGGTGCTCAACTGTG	200	NR_029476
hpri-LET7A1-A	TGTACAATTAGTTAACTGACTTTC		

Table S3:

List of specific genes extracted from ZAM zone after a transcriptomic analysis

log2 FC<2.8	log2 FC>2.8
A2M	ABCC2
AADAC	ABHD11-AS1
ABCA1	ADRB2
ABP1	AFF2
ACVRL1	AHNAK2
ADA	ANK3
ADAM12	ANO1-AS2
ADAM19	AP1S3
ADAMTS1	ARHGEF37
ADAMTS4	ATP12A
ADAMTS5	AVPR1A
ADAMTS8	BCKDHB
ADCY1	BCL11A
AGT	BSPRY
AKAP12	BZRAP1
ALDH2	C12orf28
AMIGO2	C14orf34
AMZ1	C15orf41
ANKRD1	C6orf15
ANTXR1	C7orf41
APOA1	C9orf167
APOBEC2	CAMK1D
APOC1	CAMSAP3
APOE	CCDC165
AQPEP	CCNB3
AR	CDHR4
ARG1	CDK5R1
ASPHD2	CLDN3
ASS1	CLEC1B
ATP13A4	CLU
AXDND1	CPS1
BCAR4	CSF3
BCORL1	CTSC
BIN2	CUBN
BMP8A	CYP21A2
C11orf20	CYP27C1
C11orf86	DEFB103B
C12orf42	DGKB

C15orf48	DNAJA4
C1orf115	DNAJC27-AS1
C1orf130	DNER
C1QTNF1	DSG1
C2CD4B	DST
C2orf72	DUOXA1
C4BPB	EMP1
C4orf26	ENPP5
C5orf46	EPB41
C7orf58	EPHA4
C8orf31	FBXO2
CABLES1	FBXO41
CACNA1A	FIGN
CACNA1C	FLJ25917
CCNO	FZD1
CD248	GABBR1
CD302	GABRB1
CD52	GABRP
CDA	GAS6
CDCA7	GJC2
CDH16	GSTO2
CDO1	GUCY1A3
CEACAM1	HIVEP1
CEACAM3	HOXA2
CEBPA	HPN
CFHR3	ID4
CHST2	ITPR3
CILP2	IZUMO2
CKMT2	KCNJ15
CLDN19	KCNMA1
CNR1	KCTD4
COL14A1	KIAA1244
COL27A1	KLHDC7B
CORO2A	KLK5
COTL1	KLK6
CPE	KRT27
CPZ	KRT6B
CSF2RB	LEP
CSH1	LGALS7
CSH2	LGR6
CSHL1	LINC00239
CSRP2	LOC100131662
CTAG1A	LOC100287314
CTNND2	LOC100505904

CTSH	LOC283070
CTSL1	LOC340335
CTSL1P8	LOC645638
CXCL12	LOC648149
CXCL14	MBOAT1
CXCR6	MTL5
CYP11A1	NCRNA00185
CYP26A1	NDRG2
CYP4B1	NOD2
DAB2IP	NR3C2
DENND2A	NTRK3
DFNA5	OCIAD2
DHRS3	OR2T10
DIO2	OR2T2
DIRC3	PDE4D
DISC1	PGBD3
DLK2	PLCD1
DLL1	POU3F3
DLX4	PP12719
DLX5	PPP1R13B
DLX6	PPP2R2B
DNAJC6	PRPH2
DOCK4	PTHLH
DPP6	RASGRF1
DSCR8	RGS9BP
DZIP1	RNF222
E2F2	RSPH1
EBF1	S100A4
EBI3	SAA2
ECM2	SCRN1
EDNRB	SEMA4D
EEPD1	SERPINB5
EFHD1	SERPINB7
EFNB1	SFN
ELTD1	SGPP2
ENG	SLIT2
ENTPD2	SORD
ENTPD3	SORT1
ENTPD8	SOX9
EPHB2	SPACA4
ERVMER34-1	SPRR2A
ESAM	TAS1R3
ESR1	TMEM159
ESYT3	TMEM52

EXOC3L4	TMSB15B
FA2H	TOB1
FABP7	TRIM29
FADS1	TUBB2B
FADS3	UPK1B
FAM105A	UPK3B
FAM153A	WFDC2
FAM153B	WNT2B
FAM43A	XLOC_001317
FAM78A	XLOC_007116
FAM83D	XLOC_010945
FBLN1	XLOC_012199
FBXL16	XLOC_012665
FBXO32	XLOC_014194
FGF2	XLOC_l2_001947
FGFBP1	XLOC_l2_006079
FGFR2	XLOC_l2_007543
FHOD3	XLOC_l2_010751
FIGNL2	ZNF474
FILIP1L	
FLJ13744	
FLJ16779	
FLJ30901	
FLJ31356	
FLJ43663	
FLT1	
FOLR1	
FOXO1	
GCM1	
GDA	
GDF15	
GDNF	
GDPD3	
GEM	
GH1	
GJC1	
GJD3	
GKN1	
GLDC	
GLIPR1	
GNLY	
GPC4	
GPR116	
GPR32	

GPR78	
GPX3	
GRIK2	
GTSF1	
GYLTL1B	
HAS3	
HERC6	
HES2	
HEXB	
HEY1	
HJURP	
HMGB3	
HMGB3P1	
HMHA1	
HN1	
HOXA11	
HOXA7	
HPCAL1	
HPGD	
HS3ST2	
HS6ST1	
HSD3B1	
HSPA12B	
HTRA4	
HYAL4	
ICAM2	
IGDCC3	
IGSF23	
IL13RA2	
IL15	
IL17D	
IL18BP	
IL18R1	
IL1RAP	
IL1RL1	
IL20RB	
IL2RB	
IL33	
IL6ST	
INHA	
INHBA	
ISM2	
ITGA1	
ITGAD	

ITGB3	
ITLN1	
ITLN2	
JAM2	
JAZF1	
KAL1	
KCNA4	
KCNJ16	
KCNJ2	
KCNK12	
KIAA1324	
KIF21A	
KISS1R	
KITLG	
KLHL5	
KLK3	
KLRC1	
KLRC4	
KLRG2	
KRT37	
LAIR2	
LAMB1	
LAMB4	
LDLR	
LGALS14	
LGSN	
LIFR	
LIMS3L	
LIN28B	
LINC00162	
LINC00221	
LINC00473	
LINGO2	
LIPG	
LITAF	
LOC100128098	
LOC100130111	
LOC100132735	
LOC100302650	
LOC100505495	
LOC100506328	
LOC100506580	
LOC100506783	
LOC100507033	

LOC100507140	
LOC100507351	
LOC100507410	
LOC100507566	
LOC100507639	
LOC100509091	
LOC100509498	
LOC100652823	
LOC144817	
LOC145820	
LOC219731	
LOC283404	
LOC284561	
LOC339524	
LOC340340	
LOC388242	
LOC388630	
LOC389634	
LOC644366	
LOC644686	
LOC645722	
LOC650226	
LOC729178	
LOC729680	
LUM	
MAGEA8	
MAPT	
MARC1	
MCAM	
MFAP3L	
MFSD2A	
MGAT5B	
MGP	
MGST1	
MIAT	
MIR205HG	
MLC1	
MMP11	
MMP7	
MPDZ	
MYCL1	
MYO16	
NAV3	
NBLA00301	

NDC80	
NFASC	
NFE2L3	
NIM1	
NKD2	
NKG7	
NLGN4X	
NLGN4Y	
NLRP7	
NOTUM	
NRCAM	
NRIP1	
NTN1	
NTN4	
OGDHL	
OLR1	
OOEP	
OSR2	
OXGR1	
PAGE4	
PALM3	
PAPLN	
PAPPA	
PAPPA2	
PAPSS2	
PARD6G	
PARM1	
PCDHB10	
PCDHB9	
PCOLCE2	
PDCD1LG2	
PDE6H	
PDE8B	
PDGFRL	
PDZD2	
PDZK1IP1	
PGF	
PKN1	
PLA2G7	
PLA2R1	
PLAC8	
PLCE1	
PLEKHH2	
PLIN1	

PLXDC1	
PNMAL1	
PNPLA3	
POLR1C	
PPAP2A	
PPAPDC3	
PPARG	
PPP4R4	
PRB3	
PRDM1	
PRG2	
PRKCE	
PROK1	
PROS1	
PSG1	
PSG10P	
PSG2	
PSG3	
PSG5	
PSG6	
PSG8	
PTGDS	
PTGER3	
PTN	
PTPN13	
PVR	
Q6TXI9	
RAB15	
RAB3B	
RASGRF2	
RASL11B	
RBM47	
RBPMS	
REN	
REPS2	
RGN	
RGPD1	
RGS16	
RNF150	
RRAD	
S100P	
SCARB1	
SCGB1D1	
SCUBE1	

SCUBE2	
SEMA5B	
SERPINB11	
SERPINB9	
SFRP1	
SH3BP4	
SH3BP5	
SLC16A6	
SLC22A18AS	
SLC25A15	
SLC44A5	
SLC4A7	
SLC6A2	
SLC6A4	
SLCO2A1	
SNAI1	
SNORD115-1	
SNORD115-23	
SNORD115-32	
SNORD115-4	
SNX10	
SOAT1	
SOD3	
SOHLH2	
SORBS1	
SPATA22	
SPDYE5	
SPINK5	
SPOCD1	
SPRR2G	
SRPX	
SSH2	
ST3GAL5	
ST8SIA1	
STAB2	
STON1-GTF2A1L	
STRA6	
SULF1	
SULF2	
SUN3	
SV2B	
SYN3	
SYNPO	

SYNPO2L	
SYT12	
TAC3	
TBC1D4	
TCF7L1	
TCF7L2	
TIMP4	
TKTL1	
TLE2	
TLE6	
TLR4	
TM4SF5	
TMEM108	
TMEM132B	
TMEM204	
TMEM59L	
TNFAIP2	
TNFSF10	
TPRXL	
TPST1	
TRH	
TRIM14	
TRIM64	
TSKU	
TSNARE1	
TSPAN5	
TSPAN8	
TTR	
UBD	
UCHL1	
VAV3	
VIPR2	
VIT	
VWCE	
WDR86	
WNK2	
WNT10B	
WNT6	
XAGE3	
XAGE5	
XLOC_001595	
XLOC_003286	
XLOC_003595	
XLOC_006705	

XLOC_006781	
XLOC_007052	
XLOC_007358	
XLOC_007370	
XLOC_007689	
XLOC_007875	
XLOC_008696	
XLOC_010962	
XLOC_011609	
XLOC_011645	
XLOC_012981	
XLOC_013541	
XLOC_014351	
XLOC_l2_000384	
XLOC_l2_004317	
XLOC_l2_007986	
XLOC_l2_009139	
XLOC_l2_009292	
XLOC_l2_009441	
XLOC_l2_009811	
XLOC_l2_010056	
XLOC_l2_012745	
ZFP57	
ZNF114	

Table S4:

List of jointly hypermethylated genes in ZAM Choriodecidua and over expressed in ZAM Amnion

AP1S3
BZRAP1
CDK5R1
DNAJA4
EPB41
FBXO41
FIGN
FZD1
GABRB1
GABRP
GJC2
LEP
NDRG2
NR3C2
POU3F3
PPP1R13B
RNF222
RSPH1
SEMA4D
SERPINB7
SORD
SOX9
TOB1
TRIM29
WFDC2
WNT2B

Table S5:

List of disease mesh-term associated with hypermethylated genes in ZAM Choriodecidua and over expressed in ZAM Amnion

MeSH-Term	MeSH-Term id(s)	p-value
Disease Attributes	C23.550.291	8,17E-05
Virilism	C23.888.971	1,52E-04
Genetic Predisposition to Disease	C23.550.291.687.500	3,24E-04
Disease Susceptibility	C23.550.291.687	4,59E-04
Disease Progression	C23.550.291.656	4,84E-04
Osteoporotic Fractures	C26.404.545	8,30E-04
Endocrine Gland Neoplasms	C19.344, C04.588.322	8,85E-04
Gliosis	C23.550.369	1,26E-03
Testicular Diseases	C12.294.829	1,49E-03
alpha-Thalassemia	C16.320.070.875.100, C15.378.071.141.150.875.100	1,50E-03
Pancreatic Neoplasms	C19.344.421, C06.301.761, C06.689.667, C04.588.274.761, C04.588.322.475	1,50E-03
Brain Neoplasms	C10.228.140.211, C10.551.240.250, C04.588.614.250.195	1,50E-03
Anuria	C13.351.968.934.070, C13.351.968.419.078, C12.777.419.078, C12.777.934.141	1,65E-03
Foot Deformities	C05.330	1,76E-03
Lymphatic Metastasis	C23.550.727.650.560, C04.697.650.560	1,78E-03
Pancreatic Diseases	C06.689	1,91E-03
Skin Neoplasms	C17.800.882, C04.588.805	1,93E-03
Neoplasms, Germ Cell and Embryonal	C04.557.465	2,06E-03
Hyperandrogenism	C16.131.939.316.129.750, C12.706.316.064.500, C13.351.875.253.064.500, C19.391.119.129.750, C13.351.875.253.129.750, C16.131.939.316.064.500, C19.391.119.064.500, C12.706.316.129.750	2,14E-03
Dementia	C10.228.140.380	2,16E-03
Kwashiorkor	C18.654.521.500.708.626.505	2,30E-03
Neurofibroma	C04.557.580.600.580	2,37E-03
Cryptorchidism	C12.294.829.258, C16.131.939.258, C19.391.829.258, C12.706.258	2,46E-03
Genital Neoplasms, Male	C12.758.409, C04.588.945.440, C12.294.260	2,55E-03
Nerve Sheath Neoplasms	C04.557.580.600	2,62E-03
Central Nervous System Neoplasms	C04.588.614.250, C10.551.240	2,68E-03
Cardio-Renal Syndrome	C13.351.968.419.780.400, C14.280.434.156, C12.777.419.780.400	2,75E-03
Sarcoma	C04.557.450.795	3,32E-03
Urogenital Abnormalities	C16.131.939	3,38E-03
Nervous System Neoplasms	C10.551	3,39E-03
Nervous System Neoplasms	C04.588.614	3,42E-03
Autoimmune Diseases	C20.111	3,44E-03
Urogenital Abnormalities	C12.706	3,45E-03
Mandibular Fractures	C26.404.750.467.441, C26.260.275.500.400.255	3,46E-03
Mandibular Diseases	C05.500.607	3,62E-03
Uremia	C13.351.968.419.936, C12.777.419.936	3,92E-03
Jaw Fractures	C26.404.750.467, C26.260.275.500.400	4,01E-03

Brain Infarction	C14.907.253.855.200, C10.228.140.300.775.200, C10.228.140.300.150.477, C14.907.253.092.477	4,03E-03
Female Athlete Triad Syndrome	C05.116.198.579.304, C19.391.240	4,11E-03
Mandibular Diseases	C07.320.610	4,14E-03
Neoplasm Metastasis	C23.550.727.650, C04.697.650	4,35E-03
Prostatic Neoplasms	C12.758.409.750, C12.294.260.750, C04.588.945.440.770, C12.294.565.625	4,49E-03
Brain Diseases	C10.228.140	4,55E-03
Sertoli Cell-Only Syndrome	C12.294.365.700.754	4,60E-03
Pathologic Processes	C23.550	4,63E-03
Osteophyte	C05.116.540.310.800	4,72E-03
Temporomandibular Joint Disorders	C05.500.607.221.897, C07.320.610.291.897, C05.550.905, C05.651.243.897, C07.678	4,75E-03
Pleural Effusion	C08.528.652	4,76E-03
Adrenocortical Adenoma	C19.344.078.265.500, C19.053.347.500.500, C19.053.098.265.500, C04.588.322.078.265.500	4,80E-03
Pseudohypoaldosteronism	C16.320.565.861.770, C13.351.968.419.815.770, C12.777.419.815.770, C18.452.648.861.770	4,84E-03
Premenstrual Syndrome	C23.550.568.968	4,84E-03
46, XX Disorders of Sex Development	C12.706.316.064, C19.391.119.064, C13.351.875.253.064, C16.131.939.316.064	4,85E-03
Craniomandibular Disorders	C05.500.607.221, C07.320.610.291, C05.651.243	4,96E-03
Osteoporosis	C05.116.198.579	5,04E-03
Prostatic Diseases	C12.294.565	5,29E-03
alpha-Thalassemia	C16.320.365.826.100, C15.378.420.826.100	5,29E-03
Neurodegenerative Diseases	C10.574	5,32E-03
Tracheomalacia	C17.300.182.895.500, C16.131.621.953.500, C08.907.796.500, C05.182.895.500	5,48E-03
Tracheobronchomalacia	C08.907.796	5,48E-03
Anhedonia	C23.888.592.604.039, C10.597.606.057	5,61E-03
Heart Septal Defects, Ventricular	C16.131.240.400.560.540, C14.280.400.560.540, C14.240.400.560.540	5,87E-03
Neurilemmoma	C04.557.580.625.650.595	6,08E-03
Genital Diseases, Male	C12.294	6,11E-03
Infertility, Male	C12.294.365.700	6,15E-03
Pseudotumor Cerebri	C10.228.140.631.750	6,16E-03
Endocrine System Diseases	C19	6,43E-03
Brain Ischemia	C14.907.253.092, C10.228.140.300.150	6,44E-03
Tooth Diseases	C07.793	6,50E-03
Respiratory Tract Diseases	C08	6,65E-03
Cholestasis	C06.130.120.135	6,80E-03
Kidney Failure, Chronic	C13.351.968.419.780.750.500, C12.777.419.780.750.500	6,82E-03
Tracheobronchomalacia	C16.131.621.953, C17.300.182.895, C05.182.895	6,84E-03
Urinary Tract Infections	C01.539.895, C13.351.968.892, C12.777.892	6,85E-03
Maxillofacial Injuries	C26.260.275.500	7,02E-03
Autoimmune Diseases of the Nervous System	C20.111.258, C10.114	7,16E-03
Encephalomyelitis, Autoimmune, Experimental	C20.111.258.625.300, C10.114.703.300, C10.314.350.250, C10.228.140.695.562.250	7,19E-03
Immune System Diseases	C20	7,22E-03
Ossification of Posterior Longitudinal Ligament	C05.116.900.480, C23.550.751.500	7,31E-03
Cerebrovascular Disorders	C10.228.140.300, C14.907.253	7,69E-03
Osteochondritis	C17.300.182.520, C05.182.520	7,77E-03
Chondrosarcoma	C04.557.450.795.300, C04.557.450.565.280	7,78E-03

Pelvic Inflammatory Disease	C01.539.635.500	8,08E-03
Neurilemmoma	C04.557.580.600.610.595, C04.557.465.625.650.595	8,20E-03
Refeeding Syndrome	C18.654.521.687	8,21E-03
Acanthosis Nigricans	C17.800.621.430.530.100	8,24E-03
Urogenital Neoplasms	C12.758	8,25E-03
Carcinoma, Basal Cell	C04.557.470.565.165, C04.557.470.200.165	8,36E-03
Nephritis, Interstitial	C12.777.419.570.643, C13.351.968.419.570.643	8,50E-03
Nervous System Autoimmune Disease, Experimental	C10.114.703, C20.111.258.625	8,55E-03
Teratocarcinoma	C04.557.465.900	8,59E-03
Hyperphosphatemia	C18.452.750.199	8,72E-03
Pelvic Infection	C01.539.635	8,72E-03
Pleural Diseases	C08.528	8,98E-03
Demyelinating Autoimmune Diseases, CNS	C10.228.140.695.562	9,11E-03
Neuroendocrine Tumors	C04.557.580.625.650	9,17E-03
Central Nervous System Diseases	C10.228	9,19E-03
Hereditary Autoinflammatory Diseases	C17.800.827.368	9,39E-03
Neuroendocrine Tumors	C04.557.465.625.650	9,42E-03
Heart Failure, Systolic	C14.280.434.676	9,56E-03
TDP-43 Proteinopathies	C10.574.950, C18.452.845.800	9,75E-03
Demyelinating Autoimmune Diseases, CNS	C10.314.350	9,83E-03
Carcinogenesis	C04.697.098, C23.550.727.098	9,88E-03
Chromosome Inversion	C23.550.210.190	9,88E-03
Esophageal and Gastric Varices	C06.552.494.414, C06.405.117.240	9,90E-03
Protozoan Infections, Animal	C03.752.625, C03.701.688, C22.674.710	9,94E-03

Table S6:

List of jointly hypermethylated genes in ZAM Amnion and over expressed in ZAM Choriodecidua

ADAMTS1	HPCAL1	OOEP
ADAMTS5	HPGD	PAGE4
ANTXR1	HSD3B1	PAPPA2
APOA1	ICAM2	PAPSS2
AR	IL15	PARD6G
ATP13A4	IL1RL1	PDCD1LG2
BIN2	IL20RB	PLEKHH2
C1orf130	ISM2	PPAP2A
C1QTNF1	ITGA1	PPAPDC3
C2CD4B	JAM2	PPARG
C7orf58	JAZF1	PPP4R4
CDA	KCNJ16	PRB3
CEACAM3	KIAA1324	PRG2
COL14A1	KITLG	PROK1
CORO2A	KLK3	PTGER3
CXCR6	LAIR2	SCARB1
CYP11A1	LGALS14	SERPINB11
DENND2A	LIFR	SLC44A5
DIO2	LINGO2	SLC6A2
DSCR8	LIPG	SOAT1
EEPD1	MAGEA8	SOHLH2
ENTPD8	MAPT	SSH2
FAM153B	MCAM	STAB2
FHOD3	MFSD2A	SV2B
FIGNL2	MMP11	TLR4
FLJ43663	MMP7	TM4SF5
GCM1	NFASC	TMEM132B
GDF15	NFE2L3	TNFSF10
GH1	NKD2	TPST1
GKN1	NKG7	TRIM14
GPC4	NLGN4X	TSKU
GTSF1	NLRP7	TSNARE1
GYLTL1B	OGDHL	TSPAN8
HMGB3	OLR1	VAV3
HN1		XAGE3
		ZFP57

Table S7:

List of disease mesh-term associated with hypermethylated genes in ZAM Amnion and over expressed in ZAM Choriodecidua

MeSH-Term	MeSH-Term id(s)	p-value
Gestational Trophoblastic Disease	C04.557.465.955.416, C04.850.908.416, C13.703.720.949.416	1,92E-08
Trophoblastic Neoplasms	C04.850.908, C13.703.720.949	2,33E-08
Trophoblastic Neoplasms	C04.557.465.955	2,35E-08
Rheumatoid Nodule	C17.300.775.099.683, C05.799.114.683, C05.550.114.154.683	4,13E-08
Pregnancy Complications, Neoplastic	C04.850, C13.703.720	5,56E-08
Hydatidiform Mole	C13.703.720.949.416.875, C04.557.465.955.416.812, C04.850.908.416.750	1,73E-07
Choriocarcinoma	C04.557.465.955.416.202, C13.703.720.949.416.218, C04.850.908.416.186	1,17E-06
Choriocarcinoma	C04.557.470.200.025.455, C04.557.465.955.207	1,19E-06
Communicable Diseases	C01.539.221	1,92E-06
Pre-Eclampsia	C13.703.395.249	6,78E-06
Pregnancy, Ectopic	C13.703.733	9,04E-06
Hypertension, Pregnancy-Induced	C13.703.395	9,34E-06
Metaplasia	C23.550.589	9,39E-06
Melanoma, Experimental	C04.557.465.625.650.510.525, C04.619.600, C04.557.580.625.650.510.525, C04.557.665.510.525	9,57E-06
Hypersensitivity, Delayed	C20.543.418	1,09E-05
Uveitis	C11.941.879	1,68E-05
Neovascularization, Pathologic	C23.550.589.500	2,39E-05
Rheumatic Diseases	C05.799	2,61E-05
Placenta Diseases	C13.703.590	3,04E-05
Tendon Injuries	C26.874	4,43E-05
Osteoarthritis, Knee	C05.799.613.500, C05.550.114.606.500	6,64E-05
Hepatitis, Autoimmune	C06.552.380.350.050, C20.111.567	6,98E-05
Dermatitis, Contact	C17.800.815.255, C17.800.174.255	7,84E-05
Infertility	C13.351.500.365	9,15E-05
Fetal Growth Retardation	C23.550.393.450, C13.703.277.370, C16.300.390	9,71E-05
Uveitis, Anterior	C11.941.879.780.880	1,26E-04
Sarcoidosis, Pulmonary	C15.604.515.827.725, C08.381.483.725	1,28E-04
Infertility, Female	C13.351.500.365.700	1,34E-04
Leukemia-Lymphoma, Adult T-Cell	C15.604.515.560.575.100, C04.557.337.428.580.100, C20.683.515.528.582.100	1,34E-04
Pregnancy Complications	C13.703	1,46E-04
Rhinitis	C08.730.674	1,56E-04
Joint Diseases	C05.550	1,60E-04
Tuberculosis, Pleural	C08.730.912, C08.528.928, C01.252.410.040.552.846.877	1,66E-04
Lichen Planus	C17.800.859.475.560	1,68E-04
Panuveitis	C11.941.879.780	1,86E-04
Sarcoidosis	C15.604.515.827	1,89E-04
Neoplasms, Germ Cell and Embryonal	C04.557.465	2,01E-04
Brain Neoplasms	C04.588.614.250.195, C10.228.140.211, C10.551.240.250	2,05E-04
Dermatitis, Allergic Contact	C17.800.815.255.100, C17.800.174.255.100, C20.543.418.150	2,21E-04
Myocarditis	C14.280.238.625	2,49E-04
Leukemia, T-Cell	C04.557.337.428.580, C20.683.515.528.582, C15.604.515.560.575	2,52E-04
Alveolar Bone Loss	C07.465.714.354.500, C05.116.264.150	2,56E-04
Otitis Media with Effusion	C09.218.705.663.683	2,74E-04
Encephalitis, Viral	C10.228.228.210.150.300, C10.228.228.245.340, C02.182.500.300, C02.290	2,92E-04
Granuloma	C15.604.515.292	2,94E-04

Arteritis	C14.907.184, C14.907.940.090	2,98E-04
Temporomandibular Joint Disorders	C05.550.905, C05.500.607.221.897, C07.678, C07.320.610.291.897, C05.651.243.897	3,01E-04
Craniomandibular Disorders	C05.500.607.221, C07.320.610.291, C05.651.243	3,19E-04
Skin Diseases, Vascular	C17.800.862	3,30E-04
Lichenoid Eruptions	C17.800.859.475	3,36E-04
Colitis	C06.405.205.265, C06.405.469.158.188	3,45E-04
Carcinoma, Merkel Cell	C04.925.216, C02.928.216, C04.557.465.625.650.240.325, C02.256.721.150, C04.557.580.625.650.240.325, C04.557.470.200.025.370.325	3,49E-04
Pleurisy	C08.730.582, C08.528.735	3,49E-04
Hemostatic Disorders	C14.907.454	3,54E-04
Giant Cell Arteritis	C14.907.940.090.530, C10.228.140.300.850.500, C14.907.184.438, C14.907.940.907.700, C10.114.875.700, C17.800.862.252, C14.907.253.946.700, C20.111.258.962.800	3,59E-04
Arthritis, Rheumatoid	C20.111.199	3,60E-04
Arthritis, Rheumatoid	C17.300.775.099, C05.799.114, C05.550.114.154	3,61E-04
Liposarcoma	C04.557.450.795.465, C04.557.450.550.420	3,66E-04
Arthritis	C05.550.114	3,75E-04
Shock, Hemorrhagic	C23.550.835.650, C23.550.414.980	3,80E-04
Demyelinating Autoimmune Diseases, CNS	C10.314.350	3,87E-04
Central Nervous System Neoplasms	C04.588.614.250, C10.551.240	4,01E-04
Hemostatic Disorders	C15.378.463.515	4,17E-04
Female Urogenital Diseases	C13.351	4,35E-04
Neoplasms, Glandular and Epithelial	C04.557.470	4,40E-04
Respiration Disorders	C08.618	4,49E-04
Encephalitozoonosis	C01.703.617.300	4,90E-04
Pituitary Neoplasms	C04.588.614.250.195.885.500.600, C10.551.240.250.700.500.500, C10.228.140.211.885.500.600, C10.228.140.617.477.600	4,97E-04
Scleroderma, Systemic	C17.800.784, C17.300.799	4,97E-04
Multiple Sclerosis, Relapsing-Remitting	C20.111.258.250.500.600, C10.114.375.500.600, C10.314.350.500.600	4,99E-04
Arbovirus Infections	C02.081	5,02E-04
Hemorrhagic Disorders	C15.378.463	5,15E-04
Nervous System Neoplasms	C10.551	5,26E-04
Multiple Sclerosis	C20.111.258.250.500, C10.114.375.500, C10.314.350.500	5,26E-04
Nervous System Neoplasms	C04.588.614	5,32E-04
Rheumatic Diseases	C17.300.775	5,33E-04
Hypothalamic Neoplasms	C10.228.140.211.885.500, C04.588.614.250.195.885.500, C10.228.140.617.477, C10.551.240.250.700.500	5,35E-04
Plaque, Atherosclerotic	C23.300.823	5,43E-04
Conjunctivitis	C11.187.183	5,54E-04
Cardiomyopathy, Dilated	C14.280.238.070, C14.280.195.160	5,55E-04
Periodontal Atrophy	C07.465.714.354	5,78E-04
Lichen Planus, Oral	C07.465.397, C17.800.859.475.560.397	5,90E-04
Bone Resorption	C05.116.264	5,91E-04
Demyelinating Autoimmune Diseases, CNS	C10.114.375, C20.111.258.250	6,38E-04
Rotavirus Infections	C02.782.791.814	6,51E-04
Pituitary Neoplasms	C19.344.609, C19.700.734, C10.228.140.617.738.675, C04.588.322.609	6,70E-04
Supratentorial Neoplasms	C04.588.614.250.195.885, C10.228.140.211.885, C10.551.240.250.700	6,73E-04
Acute Coronary Syndrome	C14.280.647.124, C23.888.646.215.500.074, C14.907.585.187.074, C14.907.585.124, C14.280.647.187.074	6,77E-04
Thymus Neoplasms	C15.604.861, C04.588.894.949	6,78E-04
Collagen Diseases	C17.300.200	7,04E-04

Hypertension	C14.907.489	7,12E-04
Polymyositis	C05.651.594.819, C10.668.491.562.575	7,17E-04
Crohn Disease	C06.405.469.432.500, C06.405.205.731.500	7,24E-04
Dysentery	C06.405.205.331, C06.405.469.300	7,34E-04
Adenoma	C04.557.470.035	7,43E-04
Bacteroidaceae Infections	C01.252.400.110	7,43E-04
Aspergillosis, Allergic Bronchopulmonary	C17.800.838.208.416.249.074, C01.703.295.328.249.074, C08.674.060, C20.543.480.680.085, C08.730.435.090, C01.703.534.090, C01.539.800.200.383.249.074, C08.381.472.850.500, C01.703.513.249.074	7,50E-04
Onchocerciasis, Ocular	C03.300.562, C03.335.508.700.750.361.699.500, C11.294.725.562	7,55E-04
Eosinophilia	C15.378.553.231	7,66E-04
Hypertrophy, Left Ventricular	C14.280.195.400, C23.300.775.250.400	7,85E-04
Genital Neoplasms, Female	C13.351.937.418	7,96E-04
Mucopolysaccharidosis VI	C18.452.648.595.600.670, C16.320.565.595.600.670, C16.320.565.202.715.670, C18.452.648.202.715.670, C17.300.550.575.670	8,05E-04
Esophageal Neoplasms	C06.405.249.205, C04.588.443.353, C06.301.371.205, C06.405.117.430, C04.588.274.476.205	9,12E-04
Genital Diseases, Female	C13.351.500	9,88E-04
Hepatitis, Chronic	C06.552.380.350	1,00E-03
Prolactinoma	C10.228.140.617.738.675.800, C04.557.470.035.625, C19.700.734.792, C19.344.609.792, C04.588.322.609.792	1,01E-03
Rupture	C26.761	1,02E-03
Encephalitis	C02.182.500, C10.228.228.210.150	1,02E-03
Thyroid Diseases	C19.874	1,02E-03
Sinusitis	C09.603.692.752, C08.730.749, C08.460.692.752	1,03E-03
Uterine Neoplasms	C13.351.500.852.762	1,05E-03
Shock, Traumatic	C26.797	1,07E-03
Mastocytoma	C04.557.450.565.465.249, C17.800.508.236	1,07E-03
Uveal Diseases	C11.941	1,08E-03
Vasculitis, Central Nervous System	C20.111.258.962	1,09E-03
Encephalomyelitis, Autoimmune, Experimental	C20.111.258.625.300, C10.314.350.250, C10.228.140.695.562.250, C10.114.703.300	1,10E-03
Slow Virus Diseases	C02.839	1,10E-03
Vasculitis, Central Nervous System	C14.907.253.946, C10.228.140.300.850, C10.114.875, C14.907.940.907	1,14E-03
Spondylarthritis	C05.116.900.853.625, C05.550.114.865	1,15E-03
Uterine Neoplasms	C04.588.945.418.948	1,16E-03
Uterine Neoplasms	C13.351.937.418.875	1,18E-03
Venous Thrombosis	C14.907.355.830.925	1,18E-03
Connective Tissue Diseases	C17.300	1,19E-03
Corneal Neovascularization	C11.204.290	1,21E-03
Glomerulonephritis, IGA	C20.111.525, C12.777.419.570.363.608, C13.351.968.419.570.363.608	1,22E-03
Cysticercosis	C03.335.190.902.185	1,28E-03
Anoxia	C23.888.852.079	1,29E-03
Digestive System Abnormalities	C06.198	1,30E-03
Autoimmune Diseases of the Nervous System	C20.111.258, C10.114	1,30E-03
Nematode Infections	C03.335.508	1,31E-03
Acquired Immunodeficiency Syndrome	C20.673.480.040, C02.839.040, C02.782.815.616.400.040, C02.800.801.400.040	1,33E-03
Spondylitis	C05.116.900.853	1,33E-03
Ascites	C23.550.081	1,34E-03
Eye Infections	C11.294	1,35E-03
Nervous System Autoimmune Disease, Experimental	C10.114.703, C20.111.258.625	1,37E-03

Bone Marrow Neoplasms	C15.378.400.200, C04.588.448.200, C15.378.190.250	1,38E-03
Encephalitis	C10.228.228.245	1,39E-03
Osteoarthritis, Hip	C05.799.613.400, C05.550.114.606.400	1,39E-03
Paracoccidioidomycosis	C01.703.700, C17.800.838.208.600, C01.703.295.600, C01.539.800.200.600	1,40E-03
Demyelinating Diseases	C10.314	1,43E-03
Growth Disorders	C23.550.393	1,43E-03
Spinal Diseases	C05.116.900	1,43E-03
Keratitis	C11.204.564	1,45E-03
Demyelinating Autoimmune Diseases, CNS	C10.228.140.695.562	1,48E-03
Suppuration	C01.539.830	1,48E-03
Uterine Diseases	C13.351.500.852	1,49E-03
Genital Neoplasms, Female	C04.588.945.418	1,50E-03
Cicatrix	C23.550.355.274	1,54E-03
Female Urogenital Diseases and Pregnancy Complications	C13	1,54E-03
Melanoma	C04.557.465.625.650.510, C04.557.580.625.650.510, C04.557.665.510	1,54E-03
Bronchitis	C08.127.446, C08.381.495.146	1,54E-03
Nevi and Melanomas	C04.557.665	1,72E-03
Ehrlichiosis	C01.252.400.825.200	1,73E-03
Neuroendocrine Tumors	C04.557.580.625.650	1,74E-03
Nasal Polyps	C09.603.557, C08.460.572, C23.300.825.557	1,75E-03
Gastroenteritis	C06.405.205	1,77E-03
Sarcopenia	C10.597.613.612.500, C23.888.592.608.612.500, C23.300.070.500.500	1,78E-03
Neuroendocrine Tumors	C04.557.465.625.650	1,79E-03
Abdominal Neoplasms	C04.588.033	1,81E-03
Wallerian Degeneration	C23.550.737.750	1,85E-03
Flavivirus Infections	C02.782.350.250	1,87E-03
Endometrial Neoplasms	C13.351.500.852.762.200	1,88E-03
Dermatitis	C17.800.174	1,91E-03
Rhinitis	C08.460.799, C09.603.799	1,92E-03
Neoplasms, Adipose Tissue	C04.557.450.550	1,93E-03
Ehrlichiosis	C01.252.400.054.160	1,98E-03
Liver Cirrhosis, Biliary	C06.552.630.400, C06.552.150.250, C06.130.120.135.250.250	1,99E-03
Shock	C23.550.835	2,00E-03
Neoplasms, Connective and Soft Tissue	C04.557.450	2,02E-03
Microsporidiosis	C01.703.617	2,04E-03
Barrett Esophagus	C06.405.117.102, C06.198.102	2,10E-03
Musculoskeletal Diseases	C05	2,11E-03
Hypereosinophilic Syndrome	C15.378.553.231.549	2,12E-03
Sarcoma	C04.557.450.795	2,15E-03
Corneal Diseases	C11.204	2,15E-03
Cardiomegaly	C14.280.195	2,16E-03
Tendinopathy	C26.874.800	2,16E-03
Biliary Tract Diseases	C06.130	2,19E-03
Brain Abscess	C01.323, C01.539.830.025.160, C10.228.140.116, C10.228.228.090	2,19E-03
Eye Infections	C01.539.375	2,22E-03
AIDS-Related Opportunistic Infections	C20.673.480.100, C01.539.597.050, C03.684.050, C02.597.050, C02.782.815.616.400.100	2,22E-03
Reoviridae Infections	C02.782.791	2,25E-03
Periodontal Diseases	C07.465.714	2,27E-03
Urogenital Neoplasms	C13.351.937	2,29E-03
Pulmonary Aspergillosis	C08.381.472.850	2,29E-03

Herpes Genitalis	C13.351.500.342, C02.800.801.350, C12.294.329, C02.256.466.382.290	2,32E-03
Prosthesis Failure	C23.550.767.865	2,33E-03
Cardiomegaly	C23.300.775.250	2,36E-03
Epiretinal Membrane	C11.768.328	2,39E-03
Osteoarthritis	C05.799.613, C05.550.114.606	2,43E-03
Adenocarcinoma	C04.557.470.200.025	2,45E-03
Bronchial Hyperreactivity	C08.127.210	2,48E-03
Endometrial Neoplasms	C04.588.945.418.948.585	2,50E-03
Pituitary Diseases	C10.228.140.617.738	2,51E-03
Leishmaniasis, Diffuse Cutaneous	C03.858.560.400.350, C17.800.838.775.560.400.350, C03.752.300.500.400.350	2,54E-03
Taeniasis	C03.335.190.902	2,56E-03
Xanthomatosis	C18.452.584.750	2,56E-03
Abdominal Pain	C23.888.646.100, C23.888.821.030	2,57E-03
Rhabdoviridae Infections	C02.782.580.830	2,59E-03
Endometrial Neoplasms	C13.351.937.418.875.200	2,60E-03
Neoplasm Metastasis	C23.550.727.650, C04.697.650	2,61E-03
Dry Eye Syndromes	C11.496.260	2,61E-03
Disease Resistance	C23.550.291.671	2,61E-03
Kashin-Beck Disease	C05.116.099.708.534	2,63E-03
Tendinopathy	C05.651.869	2,66E-03
Placenta Accreta	C13.703.420.643, C13.703.590.609	2,72E-03
Skin Diseases, Eczematous	C17.800.815	2,73E-03
Aggressive Periodontitis	C07.465.714.533.161	2,77E-03
Pyometra	C13.351.500.852.544	2,81E-03
Anaplasmataceae Infections	C01.252.400.054	2,84E-03
Periapical Periodontitis	C07.465.714.306.700, C07.465.714.533.487, C07.320.830.700	2,88E-03
Vasculitis	C14.907.940	2,90E-03
Mononegavirales Infections	C02.782.580	2,94E-03
Multiple Myeloma	C15.378.463.515.460, C14.907.454.460, C20.683.780.650, C15.378.147.780.650	2,97E-03
Trophoblastic Tumor, Placental Site	C04.850.908.416.186.875, C04.557.465.955.207.875, C04.557.465.955.416.202.875, C13.703.720.949.416.218.875, C04.557.470.200.025.455.875	3,00E-03
Graves Ophthalmopathy	C11.270.842, C20.111.555.500, C19.874.397.370.500, C19.874.283.605.500, C11.675.349.500.500	3,03E-03
Obstetric Labor Complications	C13.703.420	3,06E-03
Shwartzman Phenomenon	C15.378.463.515.810, C14.907.454.810, C14.907.940.890	3,09E-03
Mandibular Diseases	C05.500.607	3,11E-03
Multiple Myeloma	C04.557.595.500, C20.683.515.845	3,12E-03
HELLP Syndrome	C13.703.395.186	3,14E-03
Dermatomyositis	C17.800.185, C10.668.491.562.575.500, C17.300.250, C05.651.594.819.500, C05.651.594.297, C10.668.491.562.150	3,18E-03
Parapsoriasis	C17.800.859.575	3,19E-03
Neoplasms, Connective Tissue	C04.557.450.565	3,23E-03
Orthomyxoviridae Infections	C02.782.620	3,23E-03
Salivary Gland Diseases	C07.465.815	3,26E-03
Secernentea Infections	C03.335.508.700	3,27E-03
Fetal Diseases	C16.300	3,30E-03
Paranasal Sinus Diseases	C08.460.692, C09.603.692	3,31E-03
Bile Duct Diseases	C06.130.120	3,31E-03
Neoplasms, Vascular Tissue	C04.557.645	3,32E-03
Esophageal Diseases	C06.405.117	3,32E-03
Alveolitis, Extrinsic Allergic	C08.381.483.125, C20.543.480.680.075, C08.674.055	3,34E-03
Graves Disease	C19.874.283.605, C19.874.397.370, C11.675.349.500, C20.111.555	3,41E-03

Neoplasms by Site	C04.588	3,48E-03
Meningitis, Bacterial	C10.228.228.507.280, C01.252.200.500, C10.228.228.180.500	3,50E-03
Fetal Diseases	C13.703.277	3,53E-03
Thrombosis	C14.907.355.830	3,54E-03
Central Nervous System Viral Diseases	C02.182, C10.228.228.210	3,55E-03
Lacrimal Apparatus Diseases	C11.496	3,55E-03
Mandibular Diseases	C07.320.610	3,56E-03
Head and Neck Neoplasms	C04.588.443	3,57E-03
Fibrosis	C23.550.355	3,58E-03
Angiolymphoid Hyperplasia with Eosinophilia	C17.800.060, C15.604.515.292.007, C15.378.553.231.085	3,59E-03
Respiratory Syncytial Virus Infections	C02.782.580.600.620.750	3,61E-03
Pituitary Diseases	C19.700	3,65E-03
Pulmonary Emphysema	C08.381.495.389.750	3,66E-03
Spinal Cord Compression	C26.819.678, C10.228.854.761	3,72E-03
Abscess	C01.539.830.025	3,74E-03
Otitis Media	C09.218.705.663	3,74E-03
Helminthiasis	C03.335	3,74E-03
Osteolysis	C05.116.264.579	3,79E-03
Testicular Hydrocele	C12.294.882	3,80E-03
Pneumovirus Infections	C02.782.580.600.620	3,82E-03
Granuloma	C23.550.382	3,84E-03
Pain	C23.888.646	3,84E-03
Arthritis, Psoriatic	C17.800.859.675.175, C05.550.114.865.800.424, C05.116.900.853.625.800.424, C05.550.114.145	3,85E-03
Abortion, Habitual	C13.703.039.089	3,85E-03
Pneumonia, Pneumocystis	C08.730.610.675, C08.730.435.700, C01.703.770.700, C01.703.534.700, C08.381.472.700, C08.381.677.675	3,86E-03
Blood Loss, Surgical	C23.550.505.300, C23.550.414.300	3,90E-03
Polyradiculoneuropathy	C20.111.258.750, C10.314.750, C10.114.750	3,93E-03
Balantidiasis	C06.405.469.452.146, C03.752.200.146, C03.432.146	3,95E-03
Signs and Symptoms, Respiratory	C23.888.852	3,98E-03
Influenza, Human	C02.782.620.365, C08.730.310	3,98E-03
Pancreatitis, Chronic	C06.689.750.830	3,99E-03
Strongylida Infections	C03.335.508.700.775	3,99E-03
X-Linked Combined Immunodeficiency Diseases	C20.673.815.500, C16.614.815.500, C16.320.322.968	4,02E-03
Signs and Symptoms	C23.888	4,03E-03
Hypertension, Pregnancy-Induced	C14.907.489.480	4,04E-03
Dog Diseases	C22.268	4,09E-03
Hypothalamic Diseases	C10.228.140.617	4,11E-03
Peritoneal Neoplasms	C04.588.274.780, C06.844.620, C06.301.780, C04.588.033.513	4,12E-03
Arthritis, Experimental	C05.550.114.015	4,12E-03
Asymptomatic Infections	C23.550.291.187.500	4,13E-03
Muscular Dystrophy, Animal	C22.595	4,13E-03
Keratitis, Herpetic	C11.294.800.475, C02.256.466.382.465, C11.204.564.425, C02.325.465	4,22E-03
Respiratory Insufficiency	C08.618.846	4,25E-03
Chagas Cardiomyopathy	C14.280.238.190, C03.752.300.900.200.190	4,27E-03
Gingival Overgrowth	C07.465.714.258.428	4,27E-03
Pneumonia	C08.381.677, C08.730.610	4,29E-03
Polyradiculoneuropathy	C10.668.829.800.750	4,31E-03
Bone Neoplasms	C04.588.149, C05.116.231	4,33E-03
Tuberculosis, Pulmonary	C08.381.922, C08.730.939, C01.252.410.040.552.846.899	4,34E-03
Synovitis	C05.550.870	4,40E-03
Paramyxoviridae Infections	C02.782.580.600	4,45E-03

Lupus Erythematosus, Cutaneous	C17.300.475, C17.800.480	4,46E-03
Pneumocystis Infections	C01.703.770	4,46E-03
Necrobiotic Disorders	C17.800.550, C17.300.200.495	4,47E-03
Paraproteinemias	C15.378.147.780	4,48E-03
Exophthalmos	C11.675.349	4,49E-03
Arteriosclerosis	C14.907.137.126	4,52E-03
Paraproteinemias	C20.683.780	4,55E-03
Stomatitis	C07.465.864	4,61E-03
Down Syndrome	C16.131.260.260, C10.597.606.643.220, C16.131.077.327, C16.320.180.260	4,62E-03
Lymphatic Metastasis	C23.550.727.650.560, C04.697.650.560	4,62E-03
Gastritis	C06.405.748.398, C06.405.205.697	4,65E-03
Neoplasms, Plasma Cell	C04.557.595	4,66E-03
Ovarian Diseases	C19.391.630	4,67E-03
Otitis	C09.218.705	4,67E-03
Ovarian Diseases	C13.351.500.056.630	4,70E-03
Bronchitis	C08.730.099	4,80E-03
Dysentery, Bacillary	C06.405.205.331.479, C06.405.469.300.479, C01.252.400.310.229	4,81E-03
Glomerulonephritis	C13.351.968.419.570.363, C12.777.419.570.363	4,82E-03
Skin Diseases, Vesiculobullous	C17.800.865	4,86E-03
Behcet Syndrome	C17.800.862.150, C07.465.075, C14.907.940.100, C11.941.879.780.880.200	4,86E-03
Necrosis	C23.550.717	4,88E-03
Systemic Vasculitis	C14.907.940.897	4,90E-03
Scrub Typhus	C01.252.400.780.850	4,94E-03
Pleural Effusion, Malignant	C08.528.694.700, C04.588.894.797.640.700, C08.785.640.700, C08.528.652.700	4,96E-03
Ulcer	C23.550.891	4,96E-03
Skin Neoplasms	C17.800.882, C04.588.805	4,97E-03
Conjunctival Diseases	C11.187	5,01E-03
Epidermolysis Bullosa	C17.800.865.410, C16.131.831.493, C17.800.804.493, C17.800.827.275	5,02E-03
Signs and Symptoms, Digestive	C23.888.821	5,02E-03
Adnexal Diseases	C13.351.500.056	5,14E-03
Meningitis	C10.228.228.507	5,15E-03
Polyomavirus Infections	C02.256.721	5,16E-03
Cough	C08.618.248, C23.888.852.293	5,17E-03
Embolism and Thrombosis	C14.907.355	5,25E-03
Rhinitis, Allergic, Perennial	C08.674.453.500, C20.543.480.680.443.500, C08.460.799.315.500, C09.603.799.315.500	5,26E-03
Myositis	C10.668.491.562	5,30E-03
Angina Pectoris	C23.888.646.215.500	5,38E-03
Eye Infections, Bacterial	C01.539.375.354, C01.252.354, C11.294.354	5,39E-03
Hip Dislocation, Congenital	C16.131.621.449, C05.660.449	5,43E-03
Arthralgia	C05.550.091, C23.888.646.130	5,44E-03
Cholestasis	C06.130.120.135	5,49E-03
Cholestasis, Intrahepatic	C06.130.120.135.250, C06.552.150	5,51E-03
Hematologic Neoplasms	C04.588.448, C15.378.400	5,68E-03
Spondylarthropathies	C05.116.900.853.625.800, C05.550.114.865.800	5,72E-03
Angina Pectoris	C14.280.647.187, C14.907.585.187	5,80E-03
Dermatitis, Seborrheic	C17.800.794.230, C17.800.174.580, C17.800.859.350, C17.800.815.580	5,81E-03
Cicatrix, Hypertrophic	C23.550.355.274.505	5,95E-03
Herpes Simplex	C02.256.466.382	6,02E-03
Neoplasms, Neuroepithelial	C04.557.470.670, C04.557.580.625.600, C04.557.465.625.600	6,08E-03
Occupational Diseases	C24	6,10E-03

Asthma	C08.381.495.108	6,10E-03
Central Nervous System Bacterial Infections	C01.252.200	6,16E-03
Myositis	C05.651.594	6,19E-03
Cranial Nerve Injuries	C26.260.237, C10.292.262, C26.915.300.400, C10.900.300.218	6,20E-03
Tooth Injuries	C26.900, C07.793.850	6,21E-03
Asthma	C20.543.480.680.095	6,27E-03
Atherosclerosis	C14.907.137.126.307	6,29E-03
Central Nervous System Infections	C10.228.228	6,36E-03
Sjogren's Syndrome	C07.465.815.929.669, C05.799.114.774, C05.550.114.154.774, C20.111.199.774, C11.496.260.719, C17.300.775.099.774	6,39E-03
Central Nervous System Bacterial Infections	C10.228.228.180	6,43E-03
Cryptogenic Organizing Pneumonia	C08.381.483.487.249, C08.381.495.146.135.140.200, C08.127.446.135.140.200	6,48E-03
Periapical Diseases	C07.320.830, C07.465.714.306	6,49E-03
Enteritis	C06.405.469.326, C06.405.205.462	6,51E-03
Asthma	C08.674.095, C08.127.108	6,55E-03
Urogenital Neoplasms	C04.588.945	6,55E-03
Autoimmune Diseases	C20.111	6,63E-03
Chondrosarcoma	C04.557.450.565.280, C04.557.450.795.300	6,70E-03
Chest Pain	C23.888.646.215	6,71E-03
Lyme Neuroborreliosis	C01.252.400.825.480.700, C01.252.400.155.569.600, C10.228.228.180.437, C01.252.200.450, C01.252.847.193.569.600	6,75E-03
Obstetric Labor, Premature	C13.703.420.491	6,83E-03
Pneumonia, Pneumococcal	C08.381.677.540.550, C01.252.620.550, C01.252.410.890.670.750, C08.730.610.540.550	6,86E-03
Male Urogenital Diseases	C12	6,87E-03
Arterial Occlusive Diseases	C14.907.137	6,90E-03
Conjunctivitis, Allergic	C11.187.183.200, C20.543.480.200	6,99E-03
Tick-Borne Diseases	C01.252.400.825	6,99E-03
Sarcoma, Kaposi	C04.557.645.750, C04.557.450.795.850, C02.256.466.860	7,03E-03
Mastocytosis	C04.557.450.565.465	7,03E-03
Neurocysticercosis	C03.335.190.902.185.550, C03.105.250.550, C10.228.228.205.250.550	7,03E-03
Hernia	C23.300.707	7,04E-03
Odontogenic Cysts	C07.320.450.670, C05.500.470.690, C04.182.089.530.690	7,05E-03
Ovarian Neoplasms	C19.344.410, C04.588.322.455	7,05E-03
Rhabditida Infections	C03.335.508.700.700	7,17E-03
Strongyloidiasis	C03.335.508.700.700.799	7,17E-03
Spondylitis, Ankylosing	C05.116.900.853.625.800.850, C05.550.069.680, C05.550.114.865.800.850	7,20E-03
Enterocolitis, Necrotizing	C06.405.205.596.700, C06.405.469.363.700	7,24E-03
Orbital Diseases	C11.675	7,26E-03
Pleural Diseases	C08.528	7,28E-03
Animal Diseases	C22	7,35E-03
Measles	C02.782.580.600.500.500	7,44E-03
Leukoencephalopathies	C10.228.140.695	7,45E-03
Bovine Virus Diarrhea-Mucosal Disease	C22.196.106, C02.782.350.675.106	7,46E-03
Environmental Illness	C21.223, C20.543.312	7,46E-03
Pregnancy, Tubal	C13.703.733.703	7,46E-03
Jaw Cysts	C05.500.470, C04.182.089.530, C07.320.450	7,58E-03
Diabetic Angiopathies	C14.907.320, C19.246.099.500	7,59E-03
Trachoma	C01.539.375.354.220.800, C01.252.354.225.800, C11.294.354.220.800, C01.252.400.210.210.800, C11.187.183.220.889, C11.204.813	7,61E-03

Lymphocytic Choriomeningitis	C10.228.228.507.700.500, C02.587.580, C02.182.550.500, C10.228.228.210.500.500, C02.782.082.580	7,64E-03
Pulmonary Eosinophilia	C08.381.750, C15.378.553.231.549.750	7,71E-03
Acute Pain	C10.597.617.088, C23.888.646.115	7,76E-03
Sleep-Wake Transition Disorders	C10.886.659.700	7,88E-03
Entropion	C11.338.443	7,88E-03
Pouchitis	C06.405.469.420.520.500, C06.405.469.326.875.500, C06.405.205.462.624.500	7,91E-03
Colic	C23.888.821.030.500, C23.888.646.100.600	7,91E-03
Xerostomia	C07.465.815.929	7,91E-03
Diabetic Retinopathy	C14.907.320.382, C19.246.099.500.382, C11.768.257	7,98E-03
Heart Valve Diseases	C14.280.484	8,02E-03
Ovarian Neoplasms	C13.351.937.418.685, C19.391.630.705, C13.351.500.056.630.705	8,04E-03
Dyspnea	C08.618.326, C23.888.852.371	8,12E-03
Bronchiolitis Obliterans	C08.127.446.135.140, C08.381.495.146.135.140	8,33E-03
Hypertrophy	C23.300.775	8,37E-03
Malaria, Cerebral	C03.105.300.500, C10.228.228.205.300.500, C03.752.530.620, C03.752.530.650.675	8,48E-03
Hookworm Infections	C03.335.508.700.775.455	8,51E-03
Abortion, Spontaneous	C13.703.039	8,56E-03
Blood Protein Disorders	C15.378.147	8,61E-03
Picornaviridae Infections	C02.782.687	8,71E-03
Muscular Dystrophy, Duchenne	C16.320.577.300, C05.651.534.500.300, C10.668.491.175.500.300, C16.320.322.562	8,72E-03
Retinitis	C11.768.773	8,77E-03
Opportunistic Infections	C01.539.597, C02.597, C03.684	8,82E-03
Dermatomycoses	C17.800.838.208, C01.539.800.200, C01.703.295	8,82E-03
Hernia, Abdominal	C23.300.707.374	8,84E-03
Carcinoma, Renal Cell	C12.758.820.750.160, C12.777.419.473.160, C13.351.937.820.535.160, C04.557.470.200.025.390, C13.351.968.419.473.160, C04.588.945.947.535.160	8,85E-03
Ankylosis	C05.550.069	8,86E-03
Leukemia, Lymphoid	C04.557.337.428, C20.683.515.528, C15.604.515.560	8,92E-03
Bronchiolitis, Viral	C02.109, C08.127.446.135.321, C08.381.495.146.135.321, C08.730.099.135.321	8,98E-03
Toxoplasmosis, Animal	C03.701.688.817, C22.674.710.817, C03.752.625.817, C03.752.250.800.110	9,06E-03
Thoracic Neoplasms	C04.588.894	9,23E-03
Intellectual Disability	C10.597.606.643	9,26E-03
Liver Cirrhosis	C06.552.630	9,28E-03
RNA Virus Infections	C02.782	9,29E-03
Superinfection	C03.684.880, C01.539.597.880, C02.597.880	9,30E-03
Disorders of Environmental Origin	C21	9,30E-03
Prostatic Neoplasms	C04.588.945.440.770, C12.294.260.750, C12.294.565.625, C12.758.409.750	9,31E-03
Pneumococcal Infections	C01.252.410.890.670	9,36E-03
Neoplasms by Histologic Type	C04.557	9,43E-03
Eye Infections, Viral	C11.294.800, C02.325	9,44E-03
Fractures, Bone	C26.404	9,46E-03
Subacute Sclerosing Panencephalitis	C10.228.228.210.150.300.600, C02.290.700, C10.228.228.245.340.700, C02.782.580.600.500.500.800, C02.182.500.300.600, C02.839.862	9,46E-03
Central Nervous System Helminthiasis	C10.228.228.205.250, C03.105.250	9,46E-03
Diabetes Mellitus	C19.246	9,50E-03
Inflammatory Bowel Diseases	C06.405.469.432, C06.405.205.731	9,56E-03
Purpura	C15.378.100.802, C23.888.885.687, C23.550.414.950	9,71E-03
Respiratory Tract Neoplasms	C08.785	9,80E-03
Intervertebral Disc Displacement	C23.300.707.952, C05.116.900.307	9,83E-03

	Lyme Disease	C01.252.400.825.480, C01.252.400.155.569, C01.252.847.193.569	9,91E-03